

## Transcriptional profiles of functionally distinct HLA<sup>DR</sup><sup>+</sup>CD38<sup>+</sup> CD8 T cells subsets from acute febrile dengue patients

Prabhat Singh<sup>1\*</sup>, Prashant Bajpai<sup>1\*</sup>, Deepti Maheshwari<sup>1</sup>, Yadya M Chawla<sup>1</sup>, Kamalvishnu Gottimukkala<sup>1</sup>, Elluri Seetharami Reddy<sup>1,2</sup>, Keshav Saini<sup>1</sup>, Kaustuv Nayak<sup>1</sup>, Sivaram Gunisetty<sup>3</sup>, Charu Aggarwal<sup>1</sup>, Shweta Jain<sup>4</sup>, Chaitanya<sup>4</sup>, Paras Singla<sup>4</sup>, Manish Soneja<sup>4</sup>, Naveet Wig<sup>4#</sup>, Kaja Murali-Krishna<sup>1,3,5#</sup>, Anmol Chandele<sup>1,#</sup>

<sup>1</sup>ICGEB-Emory Vaccine Center, International Centre for Genetic Engineering and Biotechnology, Aruna Asaf Ali Marg, New Delhi, India.

<sup>2</sup> Kusuma school of biological sciences, Indian Institute of Technology Delhi, New Delhi, India.

<sup>3</sup>Dept of Pediatrics, Emory University School of Medicine, Emory University, Atlanta, GA, USA.

<sup>4</sup>Dept of Medicine, All India Institute of Medical Sciences, Ansari Nagar, New Delhi, India.

<sup>5</sup>Emory Vaccine Center, Emory University, Atlanta, GA, USA

increasing seniority.

\* Co-corresponding authors:

Anmol Chandele,

Group Leader,

## ICGEB-Emory Vaccine Center,

International Centre for Genetic Engineering and Biotechnology,

New Delhi,

India

chandeleanmol@gmail.com

30 Murali-Krishna Kaja, Associate Prof.

31 Dept of Pediatrics,

32 Emory University School of Medicine,

33 Emory University, Atlanta, GA, USA.

34 [Murali.Kaja@emory.edu](mailto:Murali.Kaja@emory.edu)

35

36 Naveet Wig, Professor

37 Dept of Medicine,

38 All India Institute of Medical Sciences,

39 New Delhi, India

40 [naveetwig@gmail.com](mailto:naveetwig@gmail.com)

41

42 **Keywords:** CD8 T cells; Dengue; Transcriptomics; IFN $\gamma$  production; human

43

44 **Running title:** Analyzing IFN $\gamma$  producing CD8 T cells in dengue.

45

46

47

48

49

50

51

52

53

54

55

56

57

58

59

60 **Abstract:**

61

62 Previous studies showed that a discrete population of the CD8 T cells with HLADR<sup>+</sup>CD38<sup>+</sup>  
63 phenotype expand massively during the acute febrile phase of dengue natural infection.  
64 Although about a third of these massively expanding HLADR<sup>+</sup>CD38<sup>+</sup> CD8 T cells were of CD69<sup>high</sup>  
65 phenotype, only a small fraction of them produced IFN $\gamma$  upon *in vitro* peptide stimulation. What  
66 other cytokines/ chemokines do these peptides stimulated HLADR<sup>+</sup>CD38<sup>+</sup> CD8 T cells express,  
67 what transcriptional profiles distinguish the CD69<sup>+</sup>IFN $\gamma$ <sup>+</sup>, CD69<sup>+</sup>IFN $\gamma$ <sup>-</sup>, and CD69<sup>-</sup>IFN $\gamma$ <sup>-</sup> subsets, and  
68 whether the expansion of the total HLADR<sup>+</sup>CD38<sup>+</sup> CD8 T cells or the IFN $\gamma$  producing CD8 T cells  
69 differ depending on disease severity remained unclear. This study addresses these knowledge  
70 gaps. We find that the CD69<sup>+</sup>IFN $\gamma$ <sup>+</sup> subset uniquely expressed key genes involved in protein  
71 translation, cellular metabolism, proliferation and dendritic cell cross talk. Both the CD69<sup>+</sup>IFN $\gamma$ <sup>+</sup>  
72 and CD69<sup>+</sup>IFN $\gamma$ <sup>-</sup> subsets had an antigen responsive gene signature with genes involved in  
73 cytotoxic effector functions, regulation of T cell receptor signaling, signaling by MAPK,  
74 chemotaxis and T cell trafficking to inflamed tissues with the expression being more robust in the  
75 IFN $\gamma$ <sup>+</sup> CD69<sup>+</sup> subset. On the other hand, the CD69<sup>-</sup>IFN $\gamma$ <sup>-</sup> subset was biased towards expression of  
76 genes that both augment and dampen T cell responses. Lastly, the expansion of total HLADR<sup>+</sup>  
77 CD38<sup>+</sup> CD8 T cells and also the IFN $\gamma$  producing HLADR<sup>+</sup>CD38<sup>+</sup> CD8 T cells was similar in patients  
78 with different grades of disease. Taken together, this study provides valuable insights into the  
79 inherent diversity of the effector CD8 T cell response during dengue.

80

81

82

83

84

85

86

87

88

89 **Introduction:**

90

91 Dengue is a global epidemic resulting in over 100 million clinically significant human cases  
92 worldwide each year with India contributing to nearly a third of the global dengue disease burden  
93 (1, 2). This mosquito borne acute systemic viral infection can result in clinical disease with  
94 symptoms ranging from mild febrile illness (dengue infection without warning signs, DI) to  
95 dengue with warning signs (DW) and severe dengue (SD), that can sometimes be life-threatening  
96 and fatal (3). Numerous studies conducted over the past several decades suggest that a multitude  
97 of host immune factors influenced by the viral-host interface, ranging from an exaggerated host  
98 innate and adaptive immune responses and inflammatory cytokines, are associated with  
99 immunopathology (4-10). Currently there is no universally licensed vaccine. Numerous vaccines  
100 are under research and evaluation and one vaccine CYD-TDV has gone through the most  
101 advanced clinical trials is licensed in some countries. This tetravalent dengue CYD-TDV vaccine  
102 expressing dengue structural proteins prM and Envelope on a yellow fever vector backbone  
103 mainly induces antibody responses since it does not carry dengue nonstructural proteins, which  
104 are major targets of the T-cell mediated response. Interestingly, this vaccine has shown  
105 demonstrable efficacy in dengue pre-immune individuals while enhancing disease in dengue  
106 naïve individuals (11) -thereby further strengthening the view point that, perhaps, vaccines that  
107 target CD8 T cells (in addition to antibody responses) may be needed for optimal protection  
108 against dengue.

109 For devising the successful vaccines, it is important to gain a detailed understanding of the human  
110 T and B cell responses and their association with protection or immunopathology during natural  
111 infection. Towards this, numerous studies revealed that while antibodies are important for  
112 protection, they can also enhance infection through a process defined as 'antibody dependent  
113 enhancement' (ADE) (4, 5, 12). Furthermore, some of the early historical studies hypothesized  
114 that cross-reactive memory T cell responses may also contribute to dengue immunopathology  
115 via mediating a "cytokine storm" that might directly or indirectly enhance disease. This

116 hypothesis was initially supported by early studies in 1990's that showed expansion of a CD69  
117 expressing CD8 T cell population peaked around the time when the patients manifested severe  
118 disease and hemorrhage (13, 14). However, several recent studies from both murine models and  
119 humans raised the possibility that the CD8 T cell responses are probably not drivers of disease  
120 severity (15-18). Therefore, there has been a renewed interest towards a detailed  
121 characterization of human CD8 T cell responses to dengue natural infection as well as to develop  
122 and evaluate vaccines that can induce both antibody and T cell responses. Previous studies from  
123 our lab and that of others showed that while there is a massive expansion of HLADR and CD38  
124 expressing CD8 T cell population in dengue patients, only a small portion of these massively  
125 expanding CD8 T cells produced IFN $\gamma$  in response to dengue peptides *ex vivo* (19-21). However,  
126 several knowledge gaps remain: What other cytokines/ chemokines do these massively  
127 expanding HLADR $^+$  CD38 $^+$  CD8 T cells express upon peptide stimulation? What transcriptional  
128 profiles distinguish the CD69 $^+$ IFN $\gamma$  $^+$ , CD69 $^+$ IFN $\gamma$  $^-$ , and CD69 $^-$ IFN $\gamma$  $^-$  populations among these  
129 massively expanding HLADR $^+$  CD38 $^+$  CD8 T cells? Does the expansion of the total HLADR $^+$ CD38 $^+$   
130 CD8 T cells or the IFN $\gamma$  producing CD8 T cells differ depending on disease severity?

131 This study addresses these questions by RNA seq analysis of the sorted HLADR $^+$ CD38 $^+$  CD8 T cells  
132 that were stimulated with dengue peptides and sorted as - CD69 $^-$ IFN $\gamma$  $^-$ , CD69 $^+$ IFN $\gamma$  $^-$  or CD69 $^+$ IFN $\gamma$  $^+$ ,  
133 and then compared to unstimulated HLADR $^+$ CD38 $^+$  CD8 T cells and to HLADR $^-$ CD38 $^-$  CD8 T cells  
134 that are enriched in naïve CD8 T cells. We found that both CD69 $^+$ IFN $\gamma$  $^-$  and CD69 $^+$ IFN $\gamma$  $^+$  subsets  
135 were very similar and were highly enriched in signatures of functional antigen reactive cytotoxic  
136 effector T cells with genes like GzmB, GzmA, Prf1, Gnly, transcription factors like Tbx21, Prdm1  
137 and co-stimulatory molecules such as TNFSF9 (4-1-BB), CD27 and ICOS. The CD69 $^+$ IFN $\gamma$  $^+$  subset  
138 not only robustly expressed these common antigen reactive cytotoxic effector gene signatures  
139 but also preferentially expressed key genes involved in protein translation, cellular metabolism,  
140 proliferation and dendritic cell cross talk and several genes of the protein translation machinery  
141 that perhaps allowed for an overall heightened expression of these antigen-responsive genes  
142 including IFN $\gamma$ . On the other hand, the bulk of the CD69 $^-$ IFN $\gamma$  $^-$  HLADR $^+$ CD38 $^+$  CD8 T cells subset  
143 expressed several cytokines and chemokines that are associated with dampening of the T cell

144 response, combined with co-stimulatory molecules and enzymes that augment T cell responses.  
145 Lastly, the total HLADR<sup>+</sup>CD38<sup>+</sup> CD8 T cells and the IFN $\gamma$  producing HLADR<sup>+</sup>CD38<sup>+</sup> CD8 T cells were  
146 similar in patients with different grades of disease severity strengthening recent studies that have  
147 de-linked CD8 T cell responses from dengue disease outcome. Taken together, this study provides  
148 valuable insights into the diversity of the effector CD8 T cell response and reveals distinct  
149 functional subsets of the massively expanding HLADR<sup>+</sup>CD38<sup>+</sup> CD8 T cells during natural dengue  
150 virus infections.

151  
152  
153  
154  
155  
156  
157  
158  
159  
160  
161  
162  
163  
164  
165  
166  
167  
168  
169  
170  
171

172

173 **Methods:**

174

175 *Human samples*

176

177 This study uses PBMC and plasma samples obtained from dengue confirmed acute febrile  
178 patients that were recruited at the Department of Medicine, All India Institute of Medical  
179 Sciences (AIIMS, New Delhi), India during the years 2018-2021. A portion of the blood sample  
180 collected for routine clinical tests at the time of enrollment, when available in sufficient quantity,  
181 was sent to research laboratory for T cell analysis. The study was approved by institutional ethical  
182 boards of the participating institutions. Informed consent was taken from enrolled participants.

183

184 *Dengue confirmation*

185

186 For dengue virus infection confirmation, Dengue NS1 Elisa (J Mitra, IR031096) and Dengue IgM  
187 Elisa (Pan Bio, 01PE20) was used in combination. Only those samples from patients who are  
188 confirmed for either dengue NS1 and/or IgM and negative for malaria (SD Bioline, 05EK40) and  
189 chikungunya (J Mitra, IR061010) were included in this study.

190

191 *Disease classification*

192

193 Disease severity grade was scored at the time of recruitment using the WHO 2009 criteria of  
194 Dengue infection without warning signs (DI), Dengue with warning signs (DW) and Severe Dengue  
195 (SD) (3).

196

197 *Whole blood processing and PBMC / plasma isolation*

198

199 The Vacutainer CPT tube (Becton Dickenson, Cat# 362761) containing blood sampling was  
200 centrifuged at 1500g for 25 minutes without brake at room temperature. After centrifugation,

201 the uppermost layer containing plasma was aspirated and then transferred to cryo-vial tubes and  
202 stored at -80°C. The white buffy coat above the gel plug containing the PBMCs was transferred  
203 to sterile 15 ml falcon tube and filled with phosphate buffered saline (PBS) (HiMedia #TL1099)  
204 and centrifuged at 1800 RPM for 8 min at 4°C. After centrifugation the supernatant was  
205 discarded, the pellet was re-suspended and washed twice in PBS. After washing, PBMC pellet was  
206 re-suspended in red blood cell lysis buffer (HiMedia Cat#R075) and incubated for 2 min to remove  
207 any remaining RBCs. The 15 ml tube was then filled with RPMI 1640 media (HiMedia #AL162S)  
208 containing 1% fetal bovine serum (FBS) and centrifuged at 1500 RPM for 5 min at 4 C and washed  
209 twice. The pellet was re-suspended in 1ml of RPMI media containing 10% FBS and the cells were  
210 counted using 0.1% trypan blue (HiMedia #TCL046). The cells were either used immediately or  
211 cryopreserved in liquid nitrogen in FBS (Hyclone #SV30014.03) with 10% dimethyl sulfoxide (MP  
212 #196055) for later analysis.

213

214 *Analytical flow cytometry*

215

216 PBMCs were washed and surface stained for 30 minutes in ice cold FACS buffer at 4°C (1xPBS  
217 containing 0.25% bovine serum albumin). Fixable viability dye e-Fluor 780 (Ebioscience,  
218 65086518) was used for excluding dead cells at the time of analysis. For CD8 T cells subsets  
219 analysis, surface staining on PBMCs was performed with CD3 (clone UCHT1), CD8 (clone SK1),  
220 CD38 (clone H1T2) and HLADR (clone L243) antibodies.

221

222 For intracellular staining, cells were fixed with fixation buffer and then permeabilized with Cytofix  
223 / Cytoperm (e-bioscience) followed by staining for 60 minutes with antibodies that were diluted  
224 in 1X perm buffer (BD, 554723). Flow cytometry data acquisition was performed either on LSR  
225 Fortessa X-20 (BD) or FACS Canto II. Data was analyzed using FlowJo software (TreeStar Inc.). CD8  
226 T cells were gated as those that co-expressed CD3 and CD8 and were analyzed of phenotypes and  
227 functions.

228

229 *Ex vivo stimulation and functional assessment of CD8 T cells*

230

231 Unless otherwise mentioned, isolated PBMCs were plated at  $1 \times 10^6$  cells/well in 96 well U-bottom  
232 plates and cultured with pool of overlapping peptides of either entire dengue proteome at a  
233 concentration of 1ug/ml of each peptide along with co-stimulation with purified anti-human  
234 CD28 (clone L293) and CD49D (clone L25). Unstimulated cells were used as negative control. As  
235 a positive control, cells were also stimulated with 1X cell stimulation cocktail containing PMA and  
236 ionomycin (Ebioscience, 00-4970-03,). Cells were then cultured for 2 hours at 37°C in 5% CO2  
237 incubator and followed by the addition of protein secretion inhibitor cocktail containing brefeldin  
238 A and monensin (GolgiPlug, BD, 555029) for another 4-hours. The cells were then harvested;  
239 surface stained with antibody cocktail containing fixable viability dye, CD3, CD8, CD38 and HLA-  
240 DR and then fixed and permeabilized using Cytofix/Cytoperm Kit. Cells were then processed for  
241 intracellular staining with antibodies against IFN $\gamma$  (clone 4S.B3), granzyme B (clone GB11) or  
242 perforin (clone deltaG9). Cells were acquired on BD Canto II or BD LSRII Fortessa X-20 and analyzed  
243 using FlowJo (TreeStar).

244

245 *IFN $\gamma$  capture assay to identify and sort IFN $\gamma$  producing CD8 T cells*

246

247 For identification and sorting of viable IFN $\gamma$  secreting cells, we used human IFN $\gamma$  secretion assay  
248 detection kit (PE) (Miltenyi Biotec, #130-054-202) as per the manufacturer's protocol. Briefly,  
249 PBMCs were cultured in 12 well flat-bottom plate and stimulated with dengue CD8 megapools  
250 (18) that were prepared at a final concentration of 1ug/ml for each peptide. Unstimulated cells  
251 were used as controls. Cells were cultured in a tissue culture incubator at 37°C for 3 hours in  
252 presence of 5% CO2. The cells were then mixed with IFN $\gamma$  catch reagent (PE conjugated anti-  
253 human IFN $\gamma$  mouse monoclonal IgG1 conjugated to anti-human CD45 mouse IgG2a). The cells  
254 were then allowed to secrete IFN $\gamma$  for an additional 45 minutes and then IFN $\gamma$  secreting cells were  
255 identified by labeling with PE-conjugated IFN $\gamma$  detection antibody (anti-human IFN $\gamma$  mouse IgG1)  
256 conjugated to PE).

257

258 *Flow cytometric cell sorting for IFN $\gamma$  producing and non-producing CD8 T cells*

259

260 After staining the cells with IFN $\gamma$  capture reagent as described in the section above, the cells were  
261 surface stained with fixable viability dye, CD3 (clone UCHT1), CD4 (clone RPA-T4 / OKT-4), CD8  
262 (clone SK1), CD38 (clone H1T2), HLADR (clone L243) and CD69 (clone FN50). Cells were then  
263 analyzed in BD FACS Aria Fusion II. After lymphocyte and doublet discrimination, we first gated  
264 on CD3 $^+$ , then excluded CD4 $^+$  cells. After this, the gated CD8 $^+$ CD3 $^+$  population was analyzed to  
265 distinguish peptide stimulated HLADR $^+$ CD38 $^+$ CD69 $^+$ IFN $\gamma$  $^+$ , peptide stimulated HLADR $^+$   
266 CD38 $^+$ CD69 $^+$ IFN $\gamma$  $^-$  and peptide stimulated HLADR $^+$ CD38 $^+$ CD69 $^-$ IFN $\gamma$  $^-$ . These CD8 T cell subsets of  
267 interest were then sorted in lysis buffer at 4°C using BD FACS aria II cell sorter. As an additional  
268 control, we also sorted the total HLADR $^+$ CD38 $^+$ CD8 T cells and HLADR $^-$ CD38 $^-$ CD8 T cells that were  
269 not stimulated with dengue peptide pool.

270

271 *RNA isolation and library preparation for RNA seq*

272

273 RNA sequencing libraries from the bulk sorted cell subsets were prepared with Illumina  
274 compatible SMARTer Stranded Total RNA-Seq Kitv2 - Pico Input Mammalian (TakaraBio, Inc.  
275 CA, USA) at Genotypic Technology Pvt. Ltd., Bangalore, India. For each condition approximately  
276 200-500 cells were sorted and collected in 10x lysis buffer of SMART-Seq v4 ultra low input RNA  
277 seq kit. From this 8 $\mu$ l was taken as input for SMARTer Stranded Total RNA-Seq Kit v2 – Pico Input  
278 Mammalian for fragmentation (with slight modification) and first strand cDNA synthesis followed  
279 by addition of illumina adaptors and indexes via 5 cycles of PCR. Indexed libraries were purified  
280 using JetSeq SPRI magnetic beads (Bio, # 68031). To remove rRNA fragments the cDNA was  
281 cleaved by ZapR with the libraries hybridized to R-probes. The resulting library fragments that  
282 were ribo-depleted were further enriched by 16-18 cycles of PCR. The final ribo-depleted libraries  
283 were purified using JetSeq SPRI magnetic beads (Bio, # 68031). The concentration of the libraries  
284 was measured using Qubit fluorometer (Thermo Fisher Scientific, MA, USA) and then analyzed  
285 on Agilent 2100 Bioanalyzer for fragment size distribution.

286

287 *RNA seq data analysis*

288

289 The transcriptome analysis was performed by processing the raw data for removal of low-quality  
290 data and adaptor sequences. The raw reads were processed using FastQC for quality assessment  
291 and pre-processing which includes removing the adapter sequences and low-quality bases (<q30)  
292 using TrimGalore. The high-quality reads were considered for alignment with reference genome  
293 using a splice aligner. Only the high-quality data was aligned to reference (Homo  
294 sapiensGRCh38.p13 build genome downloaded from Ensembl database) using Hisat2 with the  
295 default settings to identify the alignment percentage. Reads were classified into aligned and  
296 unaligned reads depending on whether they aligned to the reference genome. Hisat2 was used  
297 to calculate raw read counts for each gene after alignment. For differential gene expression  
298 analysis, low counts genes with a mean raw read count < 100 per subset were excluded. All  
299 differential gene expression analysis was performed using R package DESeq2. Genes with  
300 Benjamini-Hochberg (B-H) adjusted p-value  $\leq 0.05$  were considered significant. Further, genes  
301 with Log2 fold change of greater than or equal to +1 were considered upregulated whereas less  
302 than or equal to -1 were considered downregulated genes. For heatmaps, log normalized counts  
303 transformed to their Z-scores were used. Z-score was calculated by subtracting normalized  
304 counts with the mean of the entire dataset and then dividing it by the standard deviation ( $\sigma$ ) of  
305 the dataset. Ward.D2 method was used for hierachal clustering which employs the sum of  
306 squares of Euclidian distances to perform clustering. R packages clusterProfiler, ggplot2 and dplyr  
307 were used for data transformation and plotting.

308

309 *Pathway enrichment analysis*

310

311 KEGG enrichment analysis was performed using the R package clusterProfiler which supports  
312 downloading the latest online version of KEGG data from its website. Pathway enrichment query  
313 was run using genome wide human annotation (org.Hs.eg.db), B-H adjusted p-value cut-off  $\leq 0.05$   
314 and minimum set size > 10.

315

316 *Statistical analysis*

317 The data was curated in MS Excel and statistical analysis was performed on GraphPad prism and  
318 by using R programming language. For analysis of groups, unpaired two-tailed t test was used  
319 and p values were interpreted as \* p≤0.05; \*\* p≤0.01; \*\*\* p≤0.001, \*\*\*\*p<0.0001.

320

321 **Results:**

322

323 ***Characterization of the CD8 T cell responses in dengue patients.***

324

325 Surface markers HLADR and CD38 are well-defined for identification of activated and expanding  
326 CD8 T cells (19, 22, 23). Previous studies including ours in children with confirmed dengue showed  
327 that the HLADR<sup>+</sup>CD38<sup>+</sup> CD8 T cells expand massively during the febrile phase. Therefore, we first  
328 asked what was the expansion of the HLADR<sup>+</sup>CD38<sup>+</sup> CD8 T cell population in dengue confirmed  
329 adult acute febrile patients (**Table 1**). Consistent with previous studies (19), we found that the  
330 HLADR<sup>+</sup>CD38<sup>+</sup> CD8 T cell population expand massively in these patients as compared to healthy  
331 (**Figure 1A**) with frequencies reaching as high as 80% of the total CD8 T cells (**Figure 1B, left**) and  
332 the absolute numbers reaching as high as a million cells / ml of the blood (**Figure 1C, right**). Also  
333 consistent with previous studies in children (19), these massively expanding HLADR<sup>+</sup>CD38<sup>+</sup> CD8 T  
334 cell population were blasting as seen by high forward scatter (FSC) and side scatter (SSC) and  
335 robustly expressed proliferating cell marker (Ki67), downregulated markers of naïve cells  
336 (CD45RA, CCR7 and CD127), upregulated inflammatory homing receptors (CX3CR1, CCR5) and  
337 upregulated several markers indicative of cytotoxic T-cell effector functions (granzyme A,  
338 granzyme B and granzylsin). Interestingly, only a small proportion of these massively expanding  
339 HLADR<sup>+</sup>CD38<sup>+</sup> CD8 T cells made IFN $\gamma$  when stimulated *in vitro* with peptide pool spanning the  
340 entire dengue proteome (**Figure 1E**). The highest frequency of the IFN $\gamma$ <sup>+</sup> cells among the gated  
341 HLADR<sup>+</sup>CD38<sup>+</sup> CD8 T population was 5% with mean  $\pm$  SEM value being  $0.75 \pm 0.18$ . While the total  
342 HLADR<sup>+</sup>CD38<sup>+</sup> CD8 T cell absolute numbers reached up to a maximum of  $1 \times 10^6$  cells /ml blood,  
343 the total IFN $\gamma$  producing HLADR<sup>+</sup>CD38<sup>+</sup> CD8 T cell absolute numbers reached only up to a  
344 maximum of  $5 \times 10^4$  cells /ml blood with mean  $\pm$  SEM: being  $4.266 \times 10^3 \pm 1.580 \times 10^3$ . Nearly a  
345 third of the HLADR<sup>+</sup>CD38<sup>+</sup> CD8 T cells expressed CD69 *ex vivo* (**Fig 1H, left**). After peptide

346 stimulation, the IFN $\gamma$  producing cells that have evolved were found among these CD69 $^{+}$  cells but  
347 the IFN $\gamma$  producing population constituted only a small fraction of these CD69 $^{+}$  cells (**Figure 1H**,  
348 **middle and right**). Taken together, these results show that while the HLADR $^{+}$ CD38 $^{+}$  cells CD8 T  
349 cells have a highly differentiated effector phenotype and expand massively with a substantial  
350 portion expressing CD69 *ex vivo*, only a small proportion of them make IFN $\gamma$  in response to *in*  
351 *vitro* stimulation with dengue peptides.

352

### 353 ***RNA sequencing of functionally distinct HLADR $^{+}$ CD38 $^{+}$ CD8 T cells***

354

355 To address what other cytokines/ chemokines do these massively expanding HLADR $^{+}$  CD38 $^{+}$  CD8  
356 T cells express upon peptide stimulation and what transcriptional profiles distinguish the  
357 CD69 $^{+}$ IFN $\gamma$  $^{+}$ , CD69 $^{+}$ IFN $\gamma$  $^{-}$ , and CD69 $^{-}$ IFN $\gamma$  $^{-}$  subsets, we stimulated PBMC of three individual  
358 patients (**Supplementary Table 1**) with dengue peptides for 3 h *in vitro* and then sorted the  
359 CD69 $^{+}$ IFN $\gamma$  $^{+}$ , CD69 $^{+}$ IFN $\gamma$  $^{-}$ , and CD69 $^{-}$ IFN $\gamma$  $^{-}$  subsets among the gated HLADR $^{+}$ CD38 $^{+}$  CD8 T cell  
360 population followed by RNA seq analysis. Because the RNA analysis cannot be performed after  
361 intracellular staining, we employed IFN $\gamma$  capture assay for identifying and sorting the CD69 $^{+}$ IFN $\gamma$   
362  $^{+}$ , CD69 $^{+}$ IFN $\gamma$  $^{-}$ , and CD69 $^{-}$ IFN $\gamma$  $^{-}$  subsets. As a control, we also sorted two other subpopulations from  
363 samples that were *in vitro* cultured in the absence of peptide stimulation from four patients.  
364 These include the total HLADR $^{+}$ CD38 $^{+}$  CD8 T cell (here after referred to as unstimulated double  
365 positive or unstim DP) and the HLADR $^{-}$ CD38 $^{-}$  CD8 T cell populations (hereafter referred to as  
366 unstimulated double negative or DN). **Figure 2A**, shows the gating strategy. The post sort purity  
367 was >96%.

368

369 The DEG's found in the unstim DP in this study was largely consistent with the DEGs with our  
370 previous microarray analysis wherein we compared *ex vivo* sorted total HLADR $^{+}$ CD38 $^{+}$  CD8 T cells  
371 from dengue febrile children versus CD45RA $^{+}$ CCR7 $^{+}$  naïve CD8 T cells from the same patients (19)  
372 (**Supplementary Table 2**). This result suggested that the transcriptional profiles of the unstim DP  
373 that were obtained after *in vitro* culture are similar to the transcriptional profiles of the *ex vivo*  
374 sorted DP.

375  
376 Principal component analysis based on 14,959 differentially expressed genes (DEGs) in one or  
377 more subsets compared to the DN subset (**Supplementary Table 3**) showed that while the DN  
378 subset formed a separate cluster from all the other subsets, the unstim DP and the stimulated  
379 CD69<sup>-</sup>IFN $\gamma$ <sup>-</sup> subsets formed an overlapping cluster whereas the stimulated CD69<sup>+</sup>IFN $\gamma$ <sup>+</sup> and  
380 CD69<sup>+</sup>IFN $\gamma$ <sup>-</sup> subsets formed distinct clusters (**Figure 2B**). This result indicated that while there  
381 were no major gene expression differences between the unstim-DP and the stimulated CD69<sup>-</sup>  
382 IFN $\gamma$ <sup>-</sup> subsets, there were major gene expression differences between the unstim-DP / stimulated  
383 CD69<sup>+</sup>IFN $\gamma$ <sup>+</sup> subsets, the stimulated CD69<sup>+</sup>IFN $\gamma$ <sup>-</sup>subset, and the stimulated CD69<sup>-</sup>IFN $\gamma$ <sup>-</sup> subset.  
384 Consistent with this, the DEGs found in the Unstim DP and the stimulated CD69<sup>-</sup>IFN $\gamma$ <sup>-</sup> subsets  
385 were similar; whereas the DEGs found in the stimulated CD69<sup>+</sup>IFN $\gamma$ <sup>-</sup> subset and the stimulated  
386 CD69<sup>+</sup>IFN $\gamma$ <sup>+</sup> subsets were distinct in numbers (**Fig 2C**), expression levels (**Fig 2D and Suppl Table**  
387 **3A**) and the significant biological pathways associated (**Fig 2E**). While some biological processes  
388 such as cell cycle / DNA replication and apoptosis were significantly upregulated in the  
389 CD69<sup>+</sup>IFN $\gamma$ <sup>+</sup> subset, processes such as cytokine-cytokine receptor interaction were preferential  
390 to the CD69<sup>+</sup>IFN $\gamma$ <sup>-</sup> subset compared to the DN (**Fig 2E**). By contrast, both the unstim DP as well as  
391 the stimulated CD69<sup>+</sup>IFN $\gamma$ <sup>-</sup> subsets showed preference to some other processes related to  
392 calcium signaling, protein digestion/ absorption, extra cellular matrix interaction, insulin  
393 secretion, cGMP-PKG and PI3K-AKT signaling. On the other hand, the unstim-DP showed  
394 preference to processes related to vascular smooth muscle contraction and cAMP signaling.  
395 Because this pathway analysis did not account for qualitative and quantitative differences  
396 between the subsets, we performed a side-by-side comparison of relative expression of select  
397 genes of interest related to cytokines/ chemokines and their receptors, cytotoxic effector  
398 functions, TCR signaling, co-stimulation, proliferation, protein translation, metabolism,  
399 transcriptional machinery and other T cell effector functions. The notable findings are elaborated  
400 in the sections below.  
401  
402 ***Differences in the expression of cytokines/chemokines and their receptors in the three***  
403 ***HLADR<sup>+</sup>CD38<sup>+</sup> CD8 T cell subsets.***

404  
405 The relative expression of the DEGs related to cytokine/ chemokines is shown in **Fig 3A and**  
406 **supplementary Table 4**. Notably, we found that the CD69<sup>+</sup>IFN $\gamma$ <sup>+</sup> subset robustly expressed two  
407 other chemokines (XCL1 and XCL2) in addition to the anti-viral cytokine IFN $\gamma$ . There was very little  
408 or no expression of any of these cytokines/ chemokines in the DN, unstim-DP, CD69<sup>-</sup>IFN $\gamma$ <sup>-</sup> and the  
409 CD69<sup>+</sup>IFN $\gamma$ <sup>-</sup> subsets. On the other hand, both the unstim-DP and the CD69<sup>-</sup>IFN $\gamma$ <sup>-</sup> subset showed a  
410 bias towards expression of CXCL13, IL-16, IL-17B, IL-19, IL-34, IL-37, IL-36RN, PDGFB, TGFA and  
411 GRN.  
412  
413 Taken together, these results show that the CD69<sup>+</sup>IFN $\gamma$ <sup>+</sup> subset robustly expressed key genes  
414 involved in anti-viral functions/ MHC class-I upregulation (IFN $\gamma$ ), dendritic cell cross talk (XCL1)  
415 (24) and migration of cells during the immunological responses (XCL2) (25). By contrast, the  
416 CD69<sup>-</sup>IFN $\gamma$ <sup>-</sup> subset expressed several other cytokines/chemokines that had other immunological  
417 relevant functions. Noteworthy amongst these were - Chemokine CXCL13 that is associated with  
418 CD8 T cell dysfunction (26); cytokines such as IL-16, that has been shown to inhibit IL-2 production  
419 and is associated with CD4 dysfunction in HIV (27); IL-17b, that promotes survival and  
420 proliferation (28); IL-19 that downregulates CTL responses in helminth infections (29); IL-34, that  
421 mediates transplant tolerance (30); IL-37, that is a potent anti-inflammatory cytokine and inhibits  
422 trained immunity (31); IL-36RN, that inhibits activation of NFkB (32); PDGFb, that promotes  
423 proliferation and survival but depresses production of IL-4, IL-5 and IFN $\gamma$  (33); TGF $\alpha$ , that acts in  
424 synergy with TGF $\beta$  to also promote proliferation and survival (34). We also observed high levels  
425 of GRN, which is a Granulin that is a key lysosomal protein that contributes to inflammation and  
426 enhances that formation of inducible Tregs (iTregs) that secrete IL-10 (35) (**Figure 3A,**  
427 **Supplementary Table 4**).  
428  
429 We also observed an increased expression of IL-18R1, IL-18RAP and CXCR3 in both the CD69<sup>+</sup>IFN $\gamma$ <sup>-</sup>  
430 and the CD69<sup>+</sup>IFN $\gamma$ <sup>+</sup> subsets. IL-18R1 is a receptor for the cytokine IL-18 that mediates IFN $\gamma$   
431 synthesis (36); IL-18RAP, is an accessory subunit of the IL-18 receptor that leads to the activation  
432 of NFkB during cell mediated immunity (37) and CXCR3, a receptor for C-X-C chemokines CXCL9,

433 CXCL10 and CXCL11 that is known to be upregulated on activated effector CD8 T cells and  
434 mediates survival and proliferation (38). By contrast, the CD69<sup>-</sup>IFN $\gamma$  subset showed better  
435 expression of cytokine receptors such as CMKLR1, a receptor for chemoattractant chemerin that  
436 augments T cell mediated cytotoxicity (39); IL-12RB1, that is a receptor for pro-inflammatory  
437 cytokines IL-12 and IL-23 (40); PTGER3, a receptor for prostaglandin E2 that is required for  
438 development of fever and has been shown to be critical for IL-17 driven inflammation (41);  
439 CSF2RB/IL-15RB1 that is a common beta chain for cytokines IL-3, IL-5 and is regarded as a marker  
440 for antigen stimulated cells (42); IL-17RE, that is a receptor for pro-inflammatory cytokine IL-17C  
441 (28) and IGF1R, a high affinity receptor for IGF1 and results in the activation of PI3K-AKT and Ras-  
442 MAPK pathways (43) (**Figure 3B, Supplementary Table 5**).

443

444 Taken together, these data show that the CD69<sup>+</sup>IFN $\gamma$ <sup>+</sup>, CD69<sup>+</sup>IFN $\gamma$ <sup>-</sup> and CD69<sup>-</sup>IFN $\gamma$ <sup>-</sup> subsets differ  
445 in expression of several cytokines, chemokines and their receptor genes that have immunological  
446 relevance and distinct functions.

447

448 ***Differences in the expression of genes related to cytotoxic effector functions in the***  
449 ***HLADR<sup>+</sup>CD38<sup>+</sup> CD8 T cell subsets***

450

451 The most striking feature of CD8 T cells is their ability to kill virally infected CD8 T cells through  
452 their cytotoxic functions. Therefore, we next asked which of the subsets of HLADR<sup>+</sup>CD38<sup>+</sup> CD8 T  
453 cells did the cytotoxic gene signature filter. We observed that several key genes associated with  
454 cytotoxic effector functions were upregulated in both CD69<sup>+</sup>IFN $\gamma$ <sup>-</sup> and CD69<sup>+</sup>IFN $\gamma$ <sup>+</sup> subsets, with  
455 the latter having more robust expression. Notable were the well-known genes involved in  
456 cytotoxic effector functions such as granzyme B (GzmB), granzyme A (GzmA), granzyme H  
457 (GzmH), perforin (Perf1), Granulysin (Gnly), Cathepsin W (CTSW); CRTAM, a gene known to  
458 promote NK cell cytotoxicity and CTL function in CD8 T cells (44); and IGF2R, a gene responsible  
459 for intracellular trafficking of lysosomal enzymes (45). By contrast no genes related to cytotoxicity  
460 filtered in the CD69<sup>-</sup>IFN $\gamma$ <sup>-</sup> subset (**Figure 4A, Supplementary Table 6**). Taken together, these

461 results indicate that both the CD69<sup>+</sup>IFN $\gamma$ <sup>+</sup> subset as well as the CD69<sup>+</sup>IFN $\gamma$ <sup>-</sup> subset are highly  
462 enriched for expression of key genes involved in cytotoxic effector functions.

463

464 ***Differences in the expression of genes involved in TCR signaling / co-stimulation in the***  
465 ***HLADR<sup>+</sup>CD38<sup>+</sup> CD8 T cell subsets***

466

467 Consistent with the cytotoxic and or cytokine effector functions, the CD69<sup>+</sup>IFN $\gamma$ <sup>+</sup> and the  
468 CD69<sup>+</sup>IFN $\gamma$ <sup>-</sup> subsets also showed robust expression of several key genes involved in TCR signaling  
469 and co-stimulation. Notable among these include TNFSF9/4-1-BBL, that is a ligand for TNFRSF9/4-  
470 1-BB (46); ICOS/CD278, that enhance T cell responses (47); HAVCR1/TIM-1, a P-selectin that  
471 regulates the expression of a number of cytokines including IL-10 (48). While JAK2 and SH2D2A  
472 that participate in T cell signaling were upregulated, balancing these, both these subsets also  
473 showed expression of inhibitor receptors Lag 3 and CTLA-4 (49); PTPN22 (50) and HAVCR2 (51),  
474 that downregulate TCR signaling; and, phosphatases such as DUSP4, that downregulate MAPK  
475 and interleukin signaling (52). Additionally, the CD69<sup>-</sup>IFN $\gamma$ <sup>+</sup> also preferentially expressed the co-  
476 stimulatory molecule TNFSF14 (53).

477

478 By contrast, the CD69<sup>-</sup>IFN $\gamma$ <sup>-</sup> subset was biased towards expression genes encoding a different set  
479 of costimulatory molecules that regulate T cell responses, CD276 (54) and CD80 (55); genes  
480 belonging to the tyrosine phosphatase family – PTPRM, that is required for cell growth (56); and  
481 PTPRF that is known to negatively regulate TCR signaling by dephosphorylation of LCK and Fyn  
482 (57). Interestingly, we also observed upregulation of genes that are required for processes  
483 important to dengue disease - Endothelin 1 (EDNRA) that plays a role in vasoconstriction (58),  
484 Claudin 5 and 6 (CLDN5 and CLDN6) that are components of tight junctions and are required for  
485 extravasation of immune cells (59) (**Figure 4B, Supplementary table 7**).

486

487 ***Differences in the expression of genes involved in transcription, translation, metabolism, and***  
488 ***proliferation in the CD69<sup>+</sup>IFN $\gamma$ <sup>+</sup> subset.***

489

490 A careful comparison of the CD69<sup>+</sup>IFN $\gamma$ <sup>+</sup> subset against all the four other populations sorted  
491 revealed 70 genes that were specifically and uniquely upregulated only in the cells that were  
492 capable of making IFN $\gamma$  in response to dengue peptides (**Figure 5, and Supplementary Table 8**).  
493 Of these were genes associated with proliferation, TCR signaling, inflammation, energy  
494 metabolism and protein translation (**Figure 5A**). Notably, genes that participate in DNA  
495 replication and proliferation; CTPS1, an enzyme responsible for conversion of UTP to CTP (60);  
496 ODC1, a rate limiting enzyme in the polyamine biosynthesis pathway (61); PAICS, a key enzyme  
497 in purine biosynthesis and PPAT, also another enzyme that is of the phosphoribosyltransferase  
498 family (62) and TFRC / CD71, a transferrin receptor known to be highly upregulated on activated  
499 and proliferating T and B cells(19, 63) (**Figure 5B, Supplementary Table 8**). It is interesting to  
500 note a recent study showed that expression of CD71 may also mark memory precursor CD8 T  
501 cells (23).

502

503 These CD69<sup>+</sup>IFN $\gamma$ <sup>+</sup> HLADR<sup>+</sup>CD38<sup>+</sup> CD8 T cells were also highly metabolically active as indicated by  
504 the distinct expression of genes such as APT13A3, a p-type ATPase; GNPDA2, an enzyme that  
505 converts glucosamine-6-phosphate to fructose-6-phosphate (64); GOT2, is known to be  
506 expressed in activated CD8 T cells and is required for amino acid metabolism and TCA cycle (65);  
507 NDUFAB1 and C12orf73, both involved in the mitochondrial respiratory chain complex (66)  
508 (**Figure 5C, Supplementary Table 8**). As enhanced cellular metabolism is an indicator for cell  
509 survival, it again suggests that the cells that are capable of making IFN $\gamma$  in response to dengue  
510 peptides are probably the lineage that survives and forms the memory CD8 T cell pool.

511

512 We also observed key genes of interest that are necessary for T cell function, such as,  
513 transcription factors ID2, that promotes survival and differentiation of CD8 T cells (67); GABPB1,  
514 an Ets transcription factor, shown to be critically responsible for antigen-stimulated T cell  
515 responses (68). Other genes associated with T cell function such as RBPJ, that augments notch  
516 signaling (69); TRIB2, involved in MAPK signaling (70); ARHGEF2, shown to promote IL-6 and TNF $\alpha$   
517 secretion (71); TNFSF14/LTg (53), that promotes co-stimulation and the SPRY1 (72), that has a  
518 dual effect on cytokine production depending on the state of the T cell were found to be robustly

519 expressed. Interestingly, we also observed that the CD69<sup>+</sup>IFN $\gamma$ <sup>+</sup> HLADR<sup>+</sup>CD38<sup>+</sup> CD8 T cells also  
520 expressed genes that probably regulate overabundance of TCR mediated immune activation.  
521 Phosphatases such as PTPN7 and PTPN11 that downregulate TCR signaling were increased (57),  
522 along with SLAMF6, that is a known immune checkpoint inhibitor (73) (**Figure 5D, Suppl Table 8**).  
523

524 Lastly, lineage commitment transcription factors of IRF4, Tbx21 (T-Bet), Prdm1 (Blimp1) and Zeb2  
525 that are well known to drive cytotoxic T cell responses (74, 75) while being upregulated in both  
526 CD69<sup>+</sup>IFN $\gamma$ <sup>+</sup> and CD69<sup>+</sup>IFN $\gamma$ <sup>+</sup>, the IFN $\gamma$  producers had significantly higher expression as compared  
527 to the CD69<sup>+</sup>IFN $\gamma$ <sup>-</sup> subset indicating that this subset was more driven towards classical cytotoxic  
528 T cell responses (**Figure 5E, Supplementary Table 8**).  
529

530 A striking observation we made in the CD69<sup>+</sup>IFN $\gamma$ <sup>+</sup> HLADR<sup>+</sup>CD38<sup>+</sup> CD8 T cells was the expression  
531 of a number of genes that were involved in protein translation such as components of the  
532 ribosome RPS29, RPL22L1 and MRPL52; ribosome biogenesis regulators such as RRS1 and UTP4;  
533 translational initiation factors EIF3B, EIF2B1 and LARP7; KARS1, a lysyl-tRNA-synthetase; ZC3H14,  
534 critically required for mRNA stability; SRSF8, required for mRNA splicing and protein chaperones  
535 SACS and DNAJB11 were all found to be highly expressed (**Figure 5F, Supplementary Table 8**).  
536

537 Taken together, this data shows that the CD69<sup>+</sup>IFN $\gamma$ <sup>-</sup> subsets were also enriched for expression  
538 of several key genes that contribute to proliferation, T cell effector function, expression of lineage  
539 commitment transcription factors and processes such as protein translation that perhaps  
540 facilitates the higher expression of genes involved in immune responses, including IFN $\gamma$ .  
541

542 **Differences in the expansion of the HLADR<sup>+</sup>CD38<sup>+</sup> CD8 T cell subsets depending on disease  
543 severity**

544 We next wondered whether the expansion of the total HLADR<sup>+</sup> CD38<sup>+</sup> CD8 T cell population or  
545 the IFN $\gamma$  producing subset among these differ between the SD, DW and DI cases (**Suppl Table 9**).  
546 Enumeration of frequency and numbers of HLADR<sup>+</sup>CD38<sup>+</sup> CD8 T cells (**Figure 6A**), or IFN $\gamma$ <sup>+</sup>

548 HLADR<sup>+</sup>CD38<sup>+</sup> CD8 T cells (**Figure 6B**) showed no statistically significant differences between the  
549 SD, DW and DI cases.

550

551 **Discussion:**

552

553 In summary, we show that a discrete population of the HLADR and CD38 expressing CD8 T cells  
554 with a highly differentiated effector phenotype expand massively during the acute febrile phase  
555 of dengue natural infection. This is consistent with previous studies. Although about a third of  
556 these massively expanding HLADR<sup>+</sup> CD38<sup>+</sup> CD8 T cells found in the peripheral blood were of  
557 CD69<sup>high</sup> phenotype, only a small fraction of them produced IFN $\gamma$  upon *in vitro* stimulation with  
558 peptide pools spanning the entire dengue proteome. We found that while these small proportion  
559 of CD69<sup>+</sup>IFN $\gamma$ <sup>+</sup> subset expressed key genes involved in protein translation, cellular metabolism,  
560 proliferation and dendritic cell cross talk; both the CD69<sup>+</sup>IFN $\gamma$ <sup>+</sup> and larger proportion of CD69<sup>+</sup>  
561 IFN $\gamma$ <sup>-</sup> subsets expressed key genes that are aligned to an antigen responsive phenotype and are  
562 involved in cytotoxic effector functions, regulation of T cell receptor signaling, regulation of  
563 signaling by MAP kinases/ IL-18 and other growth factors, chemotaxis and T cell trafficking to  
564 inflamed tissues with the expression being highest in the CD69<sup>+</sup>IFN $\gamma$ <sup>+</sup> subset. Additionally, we  
565 show that the CD69<sup>-</sup>IFN $\gamma$ <sup>-</sup> subset which is the bulk of the HLADR<sup>+</sup>CD38<sup>+</sup> population expressed key  
566 cytokine/ chemokine genes that are typically implicated in dampening the immune response  
567 including those that are associated with CD8 T cell dysfunction, inhibition of IL-2 production, IL-  
568 25 signaling, NFKB activation, IL-4, IL-5, IFN $\gamma$  production; down regulation of T cell responses, and  
569 promoting the formation of the inducible T-reg. The expression of these immunoregulators in  
570 the CD69<sup>-</sup>IFN $\gamma$ <sup>-</sup> subset is likely to be constitutive and unlikely to require *in vitro* peptide  
571 stimulation since the expression of these same genes was also observed in the unstimulated  
572 HLADR<sup>+</sup>CD38<sup>+</sup> CD8 T cells (of which, nearly third of the cells are likely to be CD69<sup>-</sup>IFN $\gamma$ <sup>-</sup>  
573 phenotype). In the peripheral blood, neither the expansion of the total HLADR<sup>+</sup>CD38<sup>+</sup> CD8 T cells  
574 nor the expansion of the IFN $\gamma$  producing population among these was significantly different  
575 between the SD, DW and DI cases. These findings provide important baseline information for  
576 future studies to interrogate the tissue location and dynamics of these different cell subsets

577 during the transition from acute febrile phase to memory / recall responses in dengue natural  
578 infection and or vaccination.

579

580 Previous studies in human hepatitis virus or cytomegalovirus natural infections and influenza/  
581 yellow fever live attenuated vaccination showed that a substantial fraction of the antigen specific  
582 CD8 T cells that expand in response to viral infection are of stunned phenotype as assessed by  
583 their inability to produce IFN $\gamma$  upon *in vitro* peptide stimulation (19, 76-78). A recent study  
584 showed that those antigen-specific CD8 T cells that are capable of expressing the IFN $\gamma$  gene upon  
585 *in vitro* peptide stimulation reliably co-express chemokines such as XCL1 and XCL2 (44). Our result  
586 showing co-expression of XCL1 and XCL2 among the IFN $\gamma$  producing cells is consistent with these  
587 previous studies and suggests that, perhaps, the cytokine functional response properties of the  
588 CD8 T cells in dengue natural infection is likely to be similar to these the other human viral  
589 infections.

590

591 Interestingly, we found that the CD69 $^+$ IFN $\gamma$  $^+$  subset, in addition to expressing the IFN $\gamma$ , XCL1, XCL2  
592 and other genes associated with cytotoxic effector functions, also upregulated several other  
593 genes that contribute to an enhanced proliferation, protein translation metabolic cellular  
594 programs involving mitochondrial respiratory chain. In this perspective, it is important to note  
595 that the development of memory T cell development involves expression of large number of  
596 metabolism related genes (23). Our results, together with these previous studies, raises an  
597 interesting question on whether the memory precursors are present in only the CD69 $^+$ IFN $\gamma$  $^+$   
598 subset which constitutes a small fraction of the massively expanding HLADR $^+$ CD38 $^+$  CD8 T cells in  
599 dengue infection whose frequencies are similar to what is expected to survive after infection is  
600 resolved (79-81). This is more likely to be the case given the observations from a recent study in  
601 people vaccinated with live attenuated dengue vaccine showing that the TCR clonotypes found  
602 among the IFN $\gamma$  producing CD8 T cells was similar at the peak of the CD8 expansion and memory  
603 phase (23). Similar studies are needed in unvaccinated and vaccinated people following dengue  
604 natural infection to understand the precursors of memory development in dengue natural  
605 infection.

606  
607 Our data shows that the expansion of the HLADR<sup>+</sup>CD38<sup>+</sup> CD8 T cells or the IFN $\gamma$  producing cells  
608 did not significantly differ between the SD versus, DW versus DI cases. This finding is consistent  
609 with a recent study showing that the expansion of the IFN $\gamma$  producing cells was similar between  
610 cases with dengue hemorrhage fever (DHF) and dengue infection (DI) (16). Additionally, this  
611 recent study also compared transcriptional profiles of the IFN $\gamma$  expressing cells in patients with  
612 different grades of disease severity and found no striking difference. Thus, this study the  
613 emerging idea that the CD8 T cells responses may be protective rather than pathological in  
614 dengue.

615  
616 The transcriptional profiles of the IFN $\gamma$  producing cells that we described in this study are also  
617 consistent with the observations from a recent dengue patient study that performed single cell  
618 transcriptomics of the IFN $\gamma$  producing versus the other CD8 T cells after peptide stimulation (16).  
619 In addition to confirming these previous studies, here we provide a detailed understanding of the  
620 unique and common transcriptional signatures associated with each of the functionally distinct  
621 subsets within the massively expanding HLADR<sup>+</sup>CD38<sup>+</sup> population in the dengue patients (i.e.,  
622 CD69<sup>-</sup>IFN $\gamma$ <sup>-</sup> versus the CD69<sup>+</sup>IFN $\gamma$ <sup>-</sup> versus the CD69<sup>+</sup>IFN $\gamma$ <sup>+</sup>subsets). These results suggest that there  
623 could be distinct functional lineages of CD8 T cells within these highly activated massively  
624 expanding HLADR<sup>+</sup>CD38<sup>+</sup> CD8 T cells. Of these three subsets, the CD69<sup>+</sup>IFN $\gamma$ <sup>+</sup> subset can be  
625 undoubtedly interpreted as antigen specific since they are responding to *in vitro* peptide  
626 stimulation. However, this CD69<sup>+</sup>IFN $\gamma$ <sup>+</sup>subset represents only a minor fraction of these massively  
627 expanding HLADR<sup>+</sup>CD38<sup>+</sup> CD8 T cells. Whether the CD69<sup>+</sup>IFN $\gamma$ <sup>-</sup>subset and the CD69<sup>-</sup>IFN $\gamma$ <sup>-</sup>subsets  
628 (which together form >90% of these massively expanding CD8 T cells) truly represent antigen  
629 specific populations or bystander responses remains to be addressed. Interestingly, a recent  
630 study by Waickman et al (23), showed that people that were vaccinated with live attenuated  
631 dengue virus (TAK-003) also elicit a massive expansion of the HLADR<sup>+</sup>CD38<sup>+</sup> CD8 T cells but only  
632 a small proportion of them make IFN $\gamma$  upon *in vitro* stimulation. Thus, studies are warranted to  
633 determine whether the massively expanding HLADR<sup>+</sup>CD38<sup>+</sup> CD8 T cells in the vaccinated  
634 individuals are also comprised of the CD69<sup>-</sup>IFN $\gamma$ <sup>-</sup>, CD69<sup>+</sup>IFN $\gamma$ <sup>-</sup>, and CD69<sup>+</sup>IFN $\gamma$ <sup>+</sup> subsets as we

635 have discovered in dengue natural infection and whether each of these subsets from the  
636 vaccinated individuals express similar transcriptional profiles as what we found in dengue natural  
637 infection; and whether the protective efficacy correlate with one or more of these individual  
638 subsets of the CD8 T cells remains to be determined.

639

640 It is interesting to note that both the CD69<sup>+</sup>IFN $\gamma$ <sup>-</sup>, and CD69<sup>+</sup>IFN $\gamma$ <sup>+</sup> subsets among these massively  
641 expanding HLADR<sup>+</sup>CD38<sup>+</sup> CD8 T cells shared a number of DEGs that are directly responsible for  
642 cytotoxic functions, chemokines and their receptors and co-stimulatory and inhibitory molecules  
643 that perfectly align with an antigen-responsive phenotype. These phenotypes were very similar  
644 to those observed in single cell analysis of Flu and CMV specific CD8 T cells (44, 82). Additionally,  
645 we found that the CD69<sup>+</sup>IFN $\gamma$ <sup>+</sup> subset expressed several unique genes. These observations raise  
646 the question on whether CD69<sup>+</sup>IFN $\gamma$ <sup>-</sup> subset also has any unique gene signature. Analysis of the  
647 DEGs that specially filter to this subset revealed only four genes—SLFN12L, TENT5C, GGA2 and  
648 F2R (PAR1) (**Supplementary table 3**). Of these, PAR1 is a high affinity receptor for activated  
649 Thrombin and studies in murine models have shown that PAR1 expression accelerates calcium  
650 mobilization, and is involved in cytotoxic T cell function. Further, T cells from PAR<sup>-/-</sup> mice have  
651 dampened cytokine producing ability suggesting that PAR1/F2R might have a role in T cell  
652 function (83). However, our data does not provide any clues towards functionality that that could  
653 be uniquely attributed to the CD69<sup>+</sup>IFN $\gamma$ <sup>-</sup> subset suggesting that there might be some degree of  
654 redundancy in the function of PAR1.

655

656 Taken together, our study while improving our understanding of CD8 T cell responses in dengue,  
657 also sheds light on the diversity of the expanding CD8 T cell population and warrants further  
658 studies to understand and examine the precise role of different functional lineages of CD8 T cells  
659 in dengue natural infection and or vaccinees.

660

661 **Data sharing:** The dengue RNA seq dataset is deposited in Gene expression omnibus (GEO) with  
662 the accession code: GSE212034. The private token number for RNA seq analysis uploaded to GEO  
663 (GSE212034) for this study is 'idynkucwbvzfjs'

664

665 **Acknowledgements:** This work was funded by Dept of Biotechnology, Govt of India, grant  
666 number: BT/PR28416/MED/29/1310/2018 and U.S. National Institutes of Health grant ICIDR  
667 1U01A/115654. We thank Aditya Rathi (ICGEB-TACF) for FACS sorting of the PBMCs. We thank  
668 Dr. Daniela Weiskopf, La Jolla Institute of Immunology for CD8 megapools. The authors thank Mr.  
669 Satendra Singh, Mr. Ajay Singh, ICGEB, New Delhi for technical support.

670

671 **Declaration of interests:**

672 The authors declare no conflict of interest.

673

674 **Contributors:**

675 Experimental work, data acquisition and analysis was performed by P.S.,  
676 P.B., E.S.R., D.M., K.S., Y.C., K.N., S.J., P.S. Conceptualization and implementation by P.S.,  
677 P.B., E.S.R., D.M., K.S., Y.C., K.N., S.J., M.S., N.W., M.K.K., A.C. Manuscript writing by P.S., P.B., M.K.K.,  
678 A.C. All authors contributed to reviewing and editing the manuscript.

679

680

681 **Legends:**

682

683 **Figure 1. Analysis of the CD8 T cell responses in acute dengue febrile patients:** (A) Example of  
684 flow cytometry plot gated on total CD8 T cell showing evaluation of the HLADR<sup>+</sup>CD38<sup>+</sup> CD8 T cells  
685 in healthy (left) and dengue febrile patient (right). (B) The scatter plots show the frequencies  
686 (percentages) of HLADR<sup>+</sup>CD38<sup>+</sup>CD8 T cells among the gated CD8 T cell population and (C) absolute

687 numbers per millilitre of blood in healthy and dengue febrile adults. **(D)** The histogram plots  
688 represents the frequency of various phenotypic markers studied. HLADR<sup>+</sup>CD38<sup>+</sup> CD8 T population  
689 is red color and all other CD8 T cells green. **(E)** Example of flow cytometry plots showing IFN $\gamma$   
690 producing HLADR<sup>+</sup>CD38<sup>+</sup>CD8 T cells in unstimulated and peptides stimulated dengue patient. **(F)**  
691 The scatter plots showing frequencies and **(G)** numbers of non-IFN $\gamma$  producing and IFN $\gamma$   
692 producing HLADR<sup>+</sup>CD38<sup>+</sup>CD8 T cells after peptide stimulation in acute dengue patients. **(H)** Flow  
693 cytometry plot shows ex-vivo expression of CD69 on HLADR<sup>+</sup>CD38<sup>+</sup> CD8 T cells (right) and in-vitro  
694 expression of CD69 and IFN $\gamma$  on HLADR<sup>+</sup>CD38<sup>+</sup> CD8 T cells with and without dengue peptide  
695 stimulation (left). In B, C, F and G each dot represents analysis of different individual. Bar  
696 represents the mean. Significance values were calculated using a two-tailed Mann Whitney's U  
697 test and are indicated by: \*\*\*\*, p $\leq$ 0.0001.

698

699 **Figure 2. Sorting of IFN $\gamma$  producing HLADR<sup>+</sup> CD38<sup>+</sup> CD8 T CD8 T cells and other activated CD8 T**

700 cells from dengue patients and their global transcriptional profiling / analysis using RNA-seq.

701 **(A)** The subsets of activated CD8 T cells were sorted using flow-cytometry based on the  
702 expression of CD38, HLADR, CD69 and IFN $\gamma$  following ex-vivo stimulation for 3 hours with and  
703 without dengue peptides. The sorting strategy and purity of sort is shown. **(B)** Principal  
704 component analysis (PCA) of five subsets, unstimulated HLADR<sup>-</sup> CD38<sup>-</sup> (DN, n= 4, grey),  
705 unstimulated HLADR<sup>+</sup> CD38<sup>+</sup> (Unstim DP, n= 4, red), stimulated HLADR<sup>+</sup>CD38<sup>+</sup> CD69<sup>-</sup>IFN $\gamma$ <sup>-</sup> (CD69<sup>-</sup>  
706 IFN $\gamma$ <sup>-</sup>, n = 3, violet), stimulated HLADR<sup>+</sup>CD38<sup>+</sup> CD69<sup>+</sup>IFN $\gamma$ <sup>-</sup> (CD69<sup>+</sup>IFN $\gamma$ <sup>-</sup>, n = 3, brown) and  
707 stimulated HLADR<sup>+</sup>CD38<sup>+</sup> CD69<sup>+</sup>IFN $\gamma$ <sup>+</sup> (CD69<sup>+</sup>IFN $\gamma$ <sup>+</sup>, n = 3, blue) based on 14,959 genes. **(C)** Volcano  
708 plots highlighting differentially expressed genes in following comparisons: Unstim DP v/s DN (first  
709 from left), CD69<sup>-</sup>IFN $\gamma$ <sup>-</sup> v/s DN (second from left), CD69<sup>+</sup>IFN $\gamma$ <sup>-</sup> v/s DN (third from left) and  
710 CD69<sup>+</sup>IFN $\gamma$ <sup>+</sup> v/s DN (right). Each dot represents a gene with log<sub>2</sub> fold change (Log<sub>2</sub>FC) on x-axis  
711 and negative log<sub>10</sub> Benjamini-Hochberg (B-H) adjusted p-value (-Log<sub>10</sub> adjusted P) on y-axis.  
712 Upregulated genes (Log<sub>2</sub>FC > 1 and adjusted p-value < 0.05) are shown in red, downregulated  
713 genes (Log<sub>2</sub>FC < -1 and adjusted p-value < 0.05) are shown in blue and genes which are not  
714 significant are shown in grey. **(D)** Heatmap showing hierachal clustering of all DEGs from the  
715 comparisons shown in **(C)** based on Ward.D2 algorithm. Normalized gene expression was

716 converted into Z-scores for plotting. **(D)** KEGG pathway enrichment of genes overexpressed in  
717 Unstim DP, CD69<sup>-</sup>IFN $\gamma$ <sup>-</sup>, CD69<sup>+</sup>IFN $\gamma$ <sup>-</sup> and CD69<sup>+</sup>IFN $\gamma$ <sup>+</sup> with respect to DN is shown. Only Selected  
718 pathways amongst significant ones (B-H adjusted p-value < 0.05) are shown. For each pathway,  
719 the intensity of the colored dot represents B-H adjusted p-value and size represents the number  
720 of overexpressed genes mapped.

721

722 **Figure 3. Key genes of interest differentially regulated in CD69<sup>-</sup>IFN $\gamma$ <sup>-</sup> subset when compared**  
723 **with CD69<sup>+</sup>IFN $\gamma$ <sup>-</sup> and CD69<sup>+</sup>IFN $\gamma$ <sup>+</sup> subsets.** Heatmap showing the expression profile of key genes  
724 of interest (left). Color gradient represents the normalized gene expression transformed into z-  
725 scores from blue (low expression) to red (high expression). For each gene, bar plots representing  
726 average normalized counts of DN, Unstim DP, CD69<sup>-</sup>IFN $\gamma$ <sup>-</sup>, CD69<sup>+</sup>IFN $\gamma$ <sup>-</sup> and CD69<sup>+</sup>IFN $\gamma$ <sup>+</sup> subsets are  
727 shown. Error bar represents standard error (SEM).

728

729 **Figure 4. Notable genes upregulated in CD69<sup>+</sup>IFN $\gamma$ <sup>-</sup> and CD69<sup>+</sup>IFN $\gamma$ <sup>+</sup> subset.** Heatmap showing  
730 the expression profile of notable genes which were upregulated in CD69<sup>+</sup>IFN $\gamma$ <sup>-</sup> and CD69<sup>+</sup>IFN $\gamma$ <sup>+</sup>  
731 subset as compared to DN (left). Genes are segregated based on their functions. Color gradient  
732 represents the normalized gene expression transformed into z-scores from blue (low expression)  
733 to red (high expression). For each gene, bar plots representing average normalized counts of DN,  
734 Unstim DP, CD69<sup>-</sup>IFN $\gamma$ <sup>-</sup>, CD69<sup>+</sup>IFN $\gamma$ <sup>-</sup> and CD69<sup>+</sup>IFN $\gamma$ <sup>+</sup> subsets are shown. Error bar represents  
735 standard error (SEM).

736

737 **Figure 5. Genes uniquely overexpressed in CD69<sup>+</sup>IFN $\gamma$ <sup>+</sup> subset categorized by function.** Heatmap  
738 showing the expression profile of genes uniquely overexpressed in CD69<sup>+</sup>IFN $\gamma$ <sup>+</sup> subset (left). The  
739 genes are categorized into putative functions such as DNA replication and proliferation,  
740 metabolism, T cell functions and protein translation. Color gradient represents the normalized  
741 gene expression transformed into z-scores from blue (low expression) to red (high expression).  
742 For each gene, bar plots representing average normalized counts of DN, Unstim DP, CD69<sup>-</sup>IFN $\gamma$ <sup>-</sup>,  
743 CD69<sup>+</sup>IFN $\gamma$ <sup>-</sup> and CD69<sup>+</sup>IFN $\gamma$ <sup>+</sup> subsets are shown. Error bar represents standard error (SEM).

744

745 **Figure 6. Comparison of CD8 T Cell response in dengue patients depending on disease severity.**

746 **(A)** The scatter plots shows frequencies (left) and number (right) of HLADR<sup>+</sup>CD38<sup>+</sup> cells among  
747 the gated CD8 T cell population in acute dengue patients classified according to different grades  
748 of disease severity. **(B)** The scatter plots showing frequencies (left) and number (right) of IFN $\gamma$   
749 producing HLADR<sup>+</sup>CD38<sup>+</sup>CD8 T cells after peptide stimulation in acute dengue patients classified  
750 according to different grades of disease severity. Bar represents the mean. Significance values  
751 are calculated using Kruskal Wallis one-way analysis of variance (ANOVA) followed by Dunn's  
752 multiple comparison test. The notation ns means not significant, with p > 0.05.

753

754 **Table 1:** Characteristics of dengue confirmed adult acute febrile patients

755

756 **Supplementary Table 1:** Characteristics of dengue confirmed adult acute febrile patients from  
757 whom DN, Unstim DP, CD69<sup>-</sup>IFN $\gamma$ <sup>-</sup>, CD69<sup>+</sup>IFN $\gamma$ <sup>-</sup> and CD69<sup>+</sup>IFN $\gamma$ <sup>+</sup> subsets were sorted.

758

759 **Supplementary Table 2:** Comparison of previous microarray analysis of gene signature of  
760 HLADR<sup>+</sup>CD38<sup>+</sup> CD8 T cells and CD45RA<sup>+</sup>CCR7<sup>+</sup> CD8 T cells from dengue confirmed children.

761

762 **Supplementary Table 3:** Total differentially expressed genes in DN, Unstim DP, CD69<sup>-</sup>IFN $\gamma$ <sup>-</sup>,  
763 CD69<sup>+</sup>IFN $\gamma$ <sup>-</sup> and CD69<sup>+</sup>IFN $\gamma$ <sup>+</sup> subsets.

764

765 **Supplementary Table 4:** Differences in the expression of cytokines/chemokines and their  
766 receptors in the HLADR<sup>+</sup>CD38<sup>+</sup> CD8 T cell subsets

767

768 **Supplementary Table 5:** Differences in the expression of cytokines/chemokines and their  
769 receptors in the HLADR<sup>+</sup>CD38<sup>+</sup> CD8 T cell subsets

770

771 **Supplementary Table 6:** Differences in the expression of genes related to cytotoxic effector  
772 functions in the HLADR<sup>+</sup>CD38<sup>+</sup> CD8 T cell subsets

773

774 **Supplementary Table 7:** Differences in the expression of genes involved in TCR signaling / co-  
775 stimulation in the HLA<sup>DR</sup><sup>+</sup>CD38<sup>+</sup> CD8 T cell subsets

776

777 **Supplementary Table 8:** Differences in the expression of genes involved in transcription,  
778 translation, metabolism, and proliferation in the CD69<sup>+</sup>IFN $\gamma$ <sup>+</sup> subset.

779 **Supplementary Table 9:** Characteristics of patients with DI, DW and SD.

780

781

782

783

784

785

786

787

788

789

790

791

792

793

794

795

796

797

798

799

800

801

802

803 **References:**

804

805 1. Bhatt S, Gething PW, Brady OJ, Messina JP, Farlow AW, Moyes CL, Drake JM, Brownstein  
806 JS, Hoen AG, Sankoh O, Myers MF, George DB, Jaenisch T, Wint GR, Simmons CP, Scott  
807 TW, Farrar JJ, Hay SI. 2013. The global distribution and burden of dengue. *Nature* 496:504-  
808 7.

809 2. Gupta E, Ballani N. 2014. Current perspectives on the spread of dengue in India. *Infect  
810 Drug Resist* 7:337-42.

811 3. WHO/TDR. 2009. *Dengue: guidelines for diagnosis, treatment, prevention and control*.

812 4. Halstead SB. 1979. In vivo enhancement of dengue virus infection in rhesus monkeys by  
813 passively transferred antibody. *J Infect Dis* 140:527-33.

814 5. Kliks SC, Nisalak A, Brandt WE, Wahl L, Burke DS. 1989. Antibody-dependent  
815 enhancement of dengue virus growth in human monocytes as a risk factor for dengue  
816 hemorrhagic fever. *Am J Trop Med Hyg* 40:444-51.

817 6. Mangada MM, Rothman AL. 2005. Altered cytokine responses of dengue-specific CD4+ T  
818 cells to heterologous serotypes. *J Immunol* 175:2676-83.

819 7. Mongkolsapaya J, Dejnirattisai W, Xu XN, Vasanawathana S, Tangthawornchaikul N,  
820 Chairunsri A, Sawasdivorn S, Duangchinda T, Dong T, Rowland-Jones S, Yenchitsomanus  
821 PT, McMichael A, Malasit P, Screaton G. 2003. Original antigenic sin and apoptosis in the  
822 pathogenesis of dengue hemorrhagic fever. *Nat Med* 9:921-7.

823 8. Pang T, Cardosa MJ, Guzman MG. 2007. Of cascades and perfect storms: the  
824 immunopathogenesis of dengue haemorrhagic fever-dengue shock syndrome (DHF/DSS).  
825 *Immunol Cell Biol* 85:43-5.

826 9. Sabin AB. 1952. Research on dengue during World War II. *Am J Trop Med Hyg* 1:30-50.

827 10. Snow GE, Haaland B, Ooi EE, Gubler DJ. 2014. Review article: Research on dengue during  
828 World War II revisited. *Am J Trop Med Hyg* 91:1203-17.

829 11. Wilder-Smith A. 2020. Dengue vaccine development: status and future. *Bundesgesundheitsblatt Gesundheitsforschung Gesundheitsschutz* 63:40-44.

830 12. Katzelnick LC, Gresh L, Halloran ME, Mercado JC, Kuan G, Gordon A, Balmaseda A, Harris  
831 E. 2017. Antibody-dependent enhancement of severe dengue disease in humans. *Science*  
832 358:929-932.

833 13. Duangchinda T, Dejnirattisai W, Vasanawathana S, Limpitikul W, Tangthawornchaikul N,  
834 Malasit P, Mongkolsapaya J, Screamton G. 2010. Immunodominant T-cell responses to  
835 dengue virus NS3 are associated with DHF. *Proc Natl Acad Sci U S A* 107:16922-7.

836 14. Dung NT, Duyen HT, Thuy NT, Ngoc TV, Chau NV, Hien TT, Rowland-Jones SL, Dong T,  
837 Farrar J, Wills B, Simmons CP. 2010. Timing of CD8+ T cell responses in relation to  
838 commencement of capillary leakage in children with dengue. *J Immunol* 184:7281-7.

839 15. Elong Ngono A, Chen HW, Tang WW, Joo Y, King K, Weiskopf D, Sidney J, Sette A, Shresta  
840 S. 2016. Protective Role of Cross-Reactive CD8 T Cells Against Dengue Virus Infection.  
841 *EBioMedicine* 13:284-293.

842 16. Grifoni A, Voic H, Yu ED, Mateus J, Yan Fung KM, Wang A, Seumois G, De Silva AD,  
843 Tennekon R, Premawansa S, Premawansa G, Tippalagama R, Wijewickrama A, Chawla A,  
844 Greenbaum J, Peters B, Pandurangan V, Weiskopf D, Sette A. 2022. Transcriptomics of  
845

846 Acute DENV-Specific CD8+ T Cells Does Not Support Qualitative Differences as Drivers of  
847 Disease Severity. *Vaccines (Basel)* 10.

848 17. Lam JH, Chua YL, Lee PX, Martinez Gomez JM, Ooi EE, Alonso S. 2017. Dengue vaccine-  
849 induced CD8+ T cell immunity confers protection in the context of enhancing, interfering  
850 maternal antibodies. *JCI Insight* 2.

851 18. Weiskopf D, Angelo MA, de Azeredo EL, Sidney J, Greenbaum JA, Fernando AN,  
852 Broadwater A, Kolla RV, De Silva AD, de Silva AM, Mattia KA, Doranz BJ, Grey HM, Shresta  
853 S, Peters B, Sette A. 2013. Comprehensive analysis of dengue virus-specific responses  
854 supports an HLA-linked protective role for CD8+ T cells. *Proc Natl Acad Sci U S A*  
855 110:E2046-53.

856 19. Chandele A, Sewatanon J, Gunisetty S, Singla M, Onlamoon N, Akondy RS, Kissick HT,  
857 Nayak K, Reddy ES, Kalam H, Kumar D, Verma A, Panda H, Wang S, Angkasekwinai N,  
858 Pattanapanyasat K, Chokephaibulkit K, Medigeshi GR, Lodha R, Kabra S, Ahmed R, Murali-  
859 Krishna K. 2016. Characterization of Human CD8 T Cell Responses in Dengue Virus-  
860 Infected Patients from India. *J Virol* 90:11259-11278.

861 20. de Matos AM, Carvalho KI, Rosa DS, Villas-Boas LS, da Silva WC, Rodrigues CL, Oliveira  
862 OM, Levi JE, Araujo ES, Pannuti CS, Luna EJ, Kallas EG. 2015. CD8+ T lymphocyte  
863 expansion, proliferation and activation in dengue fever. *PLoS Negl Trop Dis* 9:e0003520.

864 21. Tian Y, Grifoni A, Sette A, Weiskopf D. 2019. Human T Cell Response to Dengue Virus  
865 Infection. *Front Immunol* 10:2125.

866 22. Akondy RS, Monson ND, Miller JD, Edupuganti S, Teuwen D, Wu H, Quyyumi F, Garg S,  
867 Altman JD, Del Rio C, Keyserling HL, Ploss A, Rice CM, Orenstein WA, Mulligan MJ, Ahmed  
868 R. 2009. The yellow fever virus vaccine induces a broad and polyfunctional human  
869 memory CD8+ T cell response. *J Immunol* 183:7919-30.

870 23. Waickman AT, Victor K, Li T, Hatch K, Rutvisuttinunt W, Medin C, Gabriel B, Jarman RG,  
871 Friberg H, Currier JR. 2019. Dissecting the heterogeneity of DENV vaccine-elicited cellular  
872 immunity using single-cell RNA sequencing and metabolic profiling. *Nat Commun*  
873 10:3666.

874 24. Matsuo K, Kitahata K, Kawabata F, Kamei M, Hara Y, Takamura S, Oiso N, Kawada A, Yoshie  
875 O, Nakayama T. 2018. A Highly Active Form of XCL1/Lymphotactin Functions as an  
876 Effective Adjuvant to Recruit Cross-Presenting Dendritic Cells for Induction of Effector and  
877 Memory CD8(+) T Cells. *Front Immunol* 9:2775.

878 25. Wang M, Windgassen D, Papoutsakis ET. 2008. Comparative analysis of transcriptional  
879 profiling of CD3+, CD4+ and CD8+ T cells identifies novel immune response players in T-  
880 cell activation. *BMC Genomics* 9:225.

881 26. Mehraj V, Ramendra R, Isnard S, Dupuy FP, Lebouche B, Costiniuk C, Thomas R, Szabo J,  
882 Baril JG, Trottier B, Cote P, LeBlanc R, Durand M, Chartrand-Lefebvre C, Kema I, Zhang Y,  
883 Finkelman M, Tremblay C, Routy JP. 2019. CXCL13 as a Biomarker of Immune Activation  
884 During Early and Chronic HIV Infection. *Front Immunol* 10:289.

885 27. Ogasawara H, Takeda-Hirokawa N, Sekigawa I, Hashimoto H, Kaneko Y, Hirose S. 1999.  
886 Inhibitory effect of interleukin-16 on interleukin-2 production by CD4+ T cells.  
887 *Immunology* 96:215-9.

888 28. Bie Q, Jin C, Zhang B, Dong H. 2017. IL-17B: A new area of study in the IL-17 family. *Mol*  
889 *Immunol* 90:50-56.

890 29. Anuradha R, Munisankar S, Dolla C, Kumaran P, Nutman TB, Babu S. 2016. Modulation of  
891 CD4+ and CD8+ T-Cell Function by Interleukin 19 and Interleukin 24 During Filarial  
892 Infections. *J Infect Dis* 213:811-5.

893 30. Bezie S, Picarda E, Ossart J, Tesson L, Usal C, Renaudin K, Anegon I, Guillonneau C. 2015.  
894 IL-34 is a Treg-specific cytokine and mediates transplant tolerance. *J Clin Invest* 125:3952-  
895 64.

896 31. Cavalli G, Tengesdal IW, Gresnigt M, Nemkov T, Arts RJW, Dominguez-Andres J, Molteni  
897 R, Stefanoni D, Cantoni E, Cassina L, Giugliano S, Schraa K, Mills TS, Pietras EM,  
898 Eisenmensser EZ, Dagna L, Boletta A, D'Alessandro A, Joosten LAB, Netea MG, Dinarello  
899 CA. 2021. The anti-inflammatory cytokine interleukin-37 is an inhibitor of trained  
900 immunity. *Cell Rep* 35:108955.

901 32. Yuan ZC, Xu WD, Liu XY, Liu XY, Huang AF, Su LC. 2019. Biology of IL-36 Signaling and Its  
902 Role in Systemic Inflammatory Diseases. *Front Immunol* 10:2532.

903 33. Daynes RA, Dowell T, Araneo BA. 1991. Platelet-derived growth factor is a potent biologic  
904 response modifier of T cells. *J Exp Med* 174:1323-33.

905 34. Lyons RM, Moses HL. 1990. Transforming growth factors and the regulation of cell  
906 proliferation. *Eur J Biochem* 187:467-73.

907 35. Wei F, Zhang Y, Zhao W, Yu X, Liu CJ. 2014. Programulin facilitates conversion and function  
908 of regulatory T cells under inflammatory conditions. *PLoS One* 9:e112110.

909 36. Tominaga K, Yoshimoto T, Torigoe K, Kurimoto M, Matsui K, Hada T, Okamura H,  
910 Nakanishi K. 2000. IL-12 synergizes with IL-18 or IL-1beta for IFN-gamma production from  
911 human T cells. *Int Immunol* 12:151-60.

912 37. Kurata R, Shimizu K, Cui X, Harada M, Isagawa T, Semba H, Ishihara J, Yamada K, Nagai J,  
913 Yoshida Y, Takeda N, Maemura K, Yonezawa T. 2020. Novel Reporter System Monitoring  
914 IL-18 Specific Signaling Can Be Applied to High-Throughput Screening. *Mar Drugs* 18.

915 38. Groom JR, Luster AD. 2011. CXCR3 in T cell function. *Exp Cell Res* 317:620-31.

916 39. Rennier K, Shin WJ, Krug E, Virdi G, Pachynski RK. 2020. Chemerin Reactivates PTEN and  
917 Suppresses PD-L1 in Tumor Cells via Modulation of a Novel CMKLR1-mediated Signaling  
918 Cascade. *Clin Cancer Res* 26:5019-5035.

919 40. Robinson RT. 2015. IL12Rbeta1: the cytokine receptor that we used to know. *Cytokine*  
920 71:348-59.

921 41. Lee J, Aoki T, Thumkeo D, Siriwatch R, Yao C, Narumiya S. 2019. T cell-intrinsic  
922 prostaglandin E2-EP2/EP4 signaling is critical in pathogenic TH17 cell-driven  
923 inflammation. *J Allergy Clin Immunol* 143:631-643.

924 42. Zhu N, Yang Y, Wang H, Tang P, Zhang H, Sun H, Gong L, Yu Z. 2022. CSF2RB Is a Unique  
925 Biomarker and Correlated With Immune Infiltrates in Lung Adenocarcinoma. *Front Oncol*  
926 12:822849.

927 43. Gusscott S, Jenkins CE, Lam SH, Giambra V, Pollak M, Weng AP. 2016. IGF1R Derived  
928 PI3K/AKT Signaling Maintains Growth in a Subset of Human T-Cell Acute Lymphoblastic  
929 Leukemias. *PLoS One* 11:e0161158.

930 44. Fuchs YF, Sharma V, Eugster A, Kraus G, Morgenstern R, Dahl A, Reinhardt S, Petzold A,  
931 Lindner A, Lobel D, Bonifacio E. 2019. Gene Expression-Based Identification of Antigen-  
932 Responsive CD8(+) T Cells on a Single-Cell Level. *Front Immunol* 10:2568.

933 45. Sohar I, Sleat D, Gong Liu C, Ludwig T, Lobel P. 1998. Mouse mutants lacking the cation-  
934 independent mannose 6-phosphate/insulin-like growth factor II receptor are impaired in  
935 lysosomal enzyme transport: comparison of cation-independent and cation-dependent  
936 mannose 6-phosphate receptor-deficient mice. *Biochem J* 330 ( Pt 2):903-8.

937 46. Croft M. 2009. The role of TNF superfamily members in T-cell function and diseases. *Nat*  
938 *Rev Immunol* 9:271-85.

939 47. Wikenheiser DJ, Stumhofer JS. 2016. ICOS Co-Stimulation: Friend or Foe? *Front Immunol*  
940 7:304.

941 48. Wang Z, Yin N, Zhang Z, Zhang Y, Zhang G, Chen W. 2017. Upregulation of T-cell  
942 Immunoglobulin and Mucin-Domain Containing-3 (Tim-3) in Monocytes/Macrophages  
943 Associates with Gastric Cancer Progression. *Immunol Invest* 46:134-148.

944 49. Blackburn SD, Shin H, Haining WN, Zou T, Workman CJ, Polley A, Betts MR, Freeman GJ,  
945 Vignali DA, Wherry EJ. 2009. Coregulation of CD8+ T cell exhaustion by multiple inhibitory  
946 receptors during chronic viral infection. *Nat Immunol* 10:29-37.

947 50. Zhang X, Yu Y, Bai B, Wang T, Zhao J, Zhang N, Zhao Y, Wang X, Wang B. 2020. PTPN22  
948 interacts with EB1 to regulate T-cell receptor signaling. *FASEB J* 34:8959-8974.

949 51. Ferris RL, Lu B, Kane LP. 2014. Too much of a good thing? Tim-3 and TCR signaling in T cell  
950 exhaustion. *J Immunol* 193:1525-30.

951 52. Sun F, Yue TT, Yang CL, Wang FX, Luo JH, Rong SJ, Zhang M, Guo Y, Xiong F, Wang CY.  
952 2021. The MAPK dual specific phosphatase (DUSP) proteins: A versatile wrestler in T cell  
953 functionality. *Int Immunopharmacol* 98:107906.

954 53. Wan X, Zhang J, Luo H, Shi G, Kapnik E, Kim S, Kanakaraj P, Wu J. 2002. A TNF family  
955 member LIGHT transduces costimulatory signals into human T cells. *J Immunol* 169:6813-  
956 21.

957 54. Liu X, Zhelev D, Adams C, Chen C, Mellors JW, Dimitrov DS. 2021. Effective killing of cells  
958 expressing CD276 (B7-H3) by a bispecific T cell engager based on a new fully human  
959 antibody. *Transl Oncol* 14:101232.

960 55. Rollins MR, Gibbons Johnson RM. 2017. CD80 Expressed by CD8(+) T Cells Contributes to  
961 PD-L1-Induced Apoptosis of Activated CD8(+) T Cells. *J Immunol Res* 2017:7659462.

962 56. Barazeghi E, Hellman P, Westin G, Stalberg P. 2019. PTPRM, a candidate tumor suppressor  
963 gene in small intestinal neuroendocrine tumors. *Endocr Connect* 8:1126-1135.

964 57. Stanford SM, Rapini N, Bottini N. 2012. Regulation of TCR signalling by tyrosine  
965 phosphatases: from immune homeostasis to autoimmunity. *Immunology* 137:1-19.

966 58. Kowalczyk A, Kleniewska P, Kolodziejczyk M, Skibská B, Goraca A. 2015. The role of  
967 endothelin-1 and endothelin receptor antagonists in inflammatory response and sepsis.  
968 *Arch Immunol Ther Exp (Warsz)* 63:41-52.

969 59. Son HJ, An CH, Yoo NJ, Lee SH. 2020. Tight Junction-Related CLDN5 and CLDN6 Genes, and  
970 Gap Junction-Related GJB6 and GJB7 Genes Are Somatically Mutated in Gastric and  
971 Colorectal Cancers. *Pathol Oncol Res* 26:1983-1987.

972 60. Martin E, Palmic N, Sanquer S, Lenoir C, Hauck F, Mongellaz C, Fabrega S, Nitschke P,  
973 Esposti MD, Schwartzentruber J, Taylor N, Majewski J, Jabado N, Wynn RF, Picard C,  
974 Fischer A, Arkwright PD, Latour S. 2014. CTP synthase 1 deficiency in humans reveals its  
975 central role in lymphocyte proliferation. *Nature* 510:288-92.

976 61. Bachmann AS, Geerts D. 2018. Polyamine synthesis as a target of MYC oncogenes. *J Biol*  
977 *Chem* 293:18757-18769.

978 62. Goswami MT, Chen G, Chakravarthi BV, Pathi SS, Anand SK, Carskadon SL, Giordano TJ,  
979 Chinnaiyan AM, Thomas DG, Palanisamy N, Beer DG, Varambally S. 2015. Role and  
980 regulation of coordinately expressed de novo purine biosynthetic enzymes PPAT and  
981 PAICS in lung cancer. *Oncotarget* 6:23445-61.

982 63. Aggarwal C, Saini K, Reddy ES, Singla M, Nayak K, Chawla YM, Maheshwari D, Singh P,  
983 Sharma P, Bhatnagar P, Kumar S, Gottimukkala K, Panda H, Gunisetty S, Davis CW, Kissick  
984 HT, Kabra SK, Lodha R, Medigeshi GR, Ahmed R, Murali-Krishna K, Chandele A. 2021.  
985 Immunophenotyping and Transcriptional Profiling of Human Plasmablasts in Dengue. *J*  
986 *Virol* 95:e0061021.

987 64. Arreola R, Valderrama B, Morante ML, Horjales E. 2003. Two mammalian glucosamine-6-  
988 phosphate deaminases: a structural and genetic study. *FEBS Lett* 551:63-70.

989 65. Hickman TL, Choi E, Whiteman KR, Muralidharan S, Pai T, Johnson T, Parikh A, Friedman  
990 T, Gilbert M, Shen B, Barron L, McGinness KE, Ettenberg SA, Motz GT, Weiss GJ, Jensen-  
991 Smith A. 2022. BOXR1030, an anti-GPC3 CAR with exogenous GOT2 expression, shows  
992 enhanced T cell metabolism and improved anti-cell line derived tumor xenograft activity.  
993 *PLoS One* 17:e0266980.

994 66. Hou T, Zhang R, Jian C, Ding W, Wang Y, Ling S, Ma Q, Hu X, Cheng H, Wang X. 2019.  
995 NDUFAB1 confers cardio-protection by enhancing mitochondrial bioenergetics through  
996 coordination of respiratory complex and supercomplex assembly. *Cell Res* 29:754-766.

997 67. Cannarile MA, Lind NA, Rivera R, Sheridan AD, Camfield KA, Wu BB, Cheung KP, Ding Z,  
998 Goldrath AW. 2006. Transcriptional regulator Id2 mediates CD8+ T cell immunity. *Nat*  
999 *Immunol* 7:1317-25.

1000 68. Luo CT, Osmanbeyoglu HU, Do MH, Bivona MR, Toure A, Kang D, Xie Y, Leslie CS, Li MO.  
1001 2017. Ets transcription factor GABP controls T cell homeostasis and immunity. *Nat*  
1002 *Commun* 8:1062.

1003 69. Lake RJ, Tsai PF, Choi I, Won KJ, Fan HY. 2014. RBPJ, the major transcriptional effector of  
1004 Notch signaling, remains associated with chromatin throughout mitosis, suggesting a role  
1005 in mitotic bookmarking. *PLoS Genet* 10:e1004204.

1006 70. Johnston J, Basatvat S, Ilyas Z, Francis S, Kiss-Toth E. 2015. Tribbles in inflammation.  
1007 *Biochem Soc Trans* 43:1069-74.

1008 71. Lu G, Tian S, Sun Y, Dong J, Wang N, Zeng J, Nie Y, Wu K, Han Y, Feng B, Shang Y. 2021.  
1009 NEK9, a novel effector of IL-6/STAT3, regulates metastasis of gastric cancer by targeting  
1010 ARHGEF2 phosphorylation. *Theranostics* 11:2460-2474.

1011 72. Choi H, Cho SY, Schwartz RH, Choi K. 2006. Dual effects of Sprouty1 on TCR signaling  
1012 depending on the differentiation state of the T cell. *J Immunol* 176:6034-45.

1013 73. Yigit B, Wang N, Ten Hacken E, Chen SS, Bhan AK, Suarez-Fueyo A, Katsuyama E, Tsokos  
1014 GC, Chiorazzi N, Wu CJ, Burger JA, Herzog RW, Engel P, Terhorst C. 2019. SLAMF6 as a  
1015 Regulator of Exhausted CD8(+) T Cells in Cancer. *Cancer Immunol Res* 7:1485-1496.

1016 74. Dominguez CX, Amezquita RA, Guan T, Marshall HD, Joshi NS, Kleinstein SH, Kaech SM.  
1017 2015. The transcription factors ZEB2 and T-bet cooperate to program cytotoxic T cell  
1018 terminal differentiation in response to LCMV viral infection. *J Exp Med* 212:2041-56.

1019 75. Joshi NS, Cui W, Chandele A, Lee HK, Urso DR, Hagman J, Gapin L, Kaech SM. 2007.  
1020 Inflammation directs memory precursor and short-lived effector CD8(+) T cell fates via  
1021 the graded expression of T-bet transcription factor. *Immunity* 27:281-95.  
1022 76. Ahmed R, Akondy RS. 2011. Insights into human CD8(+) T-cell memory using the yellow  
1023 fever and smallpox vaccines. *Immunol Cell Biol* 89:340-5.  
1024 77. Lechner F, Wong DK, Dunbar PR, Chapman R, Chung RT, Dohrenwend P, Robbins G,  
1025 Phillips R, Kleenerman P, Walker BD. 2000. Analysis of successful immune responses in  
1026 persons infected with hepatitis C virus. *J Exp Med* 191:1499-512.  
1027 78. Welsh RM. 2001. Assessing CD8 T cell number and dysfunction in the presence of antigen.  
1028 *J Exp Med* 193:F19-22.  
1029 79. Kaech SM, Hemby S, Kersh E, Ahmed R. 2002. Molecular and functional profiling of  
1030 memory CD8 T cell differentiation. *Cell* 111:837-51.  
1031 80. Kaech SM, Tan JT, Wherry EJ, Konieczny BT, Surh CD, Ahmed R. 2003. Selective expression  
1032 of the interleukin 7 receptor identifies effector CD8 T cells that give rise to long-lived  
1033 memory cells. *Nat Immunol* 4:1191-8.  
1034 81. Kaech SM, Wherry EJ. 2007. Heterogeneity and cell-fate decisions in effector and memory  
1035 CD8+ T cell differentiation during viral infection. *Immunity* 27:393-405.  
1036 82. Chng MHY, Lim MQ, Rouers A, Becht E, Lee B, MacAry PA, Lye DC, Leo YS, Chen J, Fink K,  
1037 Rivino L, Newell EW. 2019. Large-Scale HLA Tetramer Tracking of T Cells during Dengue  
1038 Infection Reveals Broad Acute Activation and Differentiation into Two Memory Cell Fates.  
1039 *Immunity* 51:1119-1135 e5.  
1040 83. Chen H, Smith M, Herz J, Li T, Hasley R, Le Saout C, Zhu Z, Cheng J, Gronda A, Martina JA,  
1041 Irusta PM, Karpova T, McGavern DB, Catalfamo M. 2021. The role of protease-activated  
1042 receptor 1 signaling in CD8 T cell effector functions. *iScience* 24:103387.  
1043

---

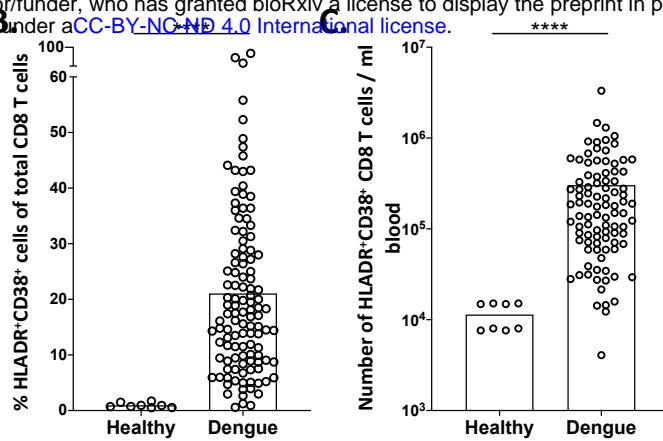
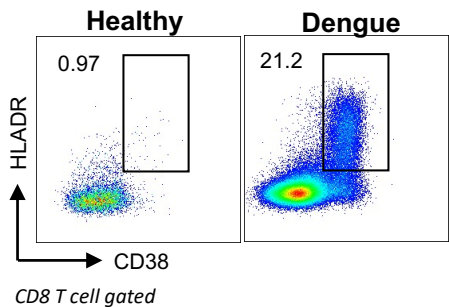
**Table 1.** Summary of dengue patients analyzed in this study

---

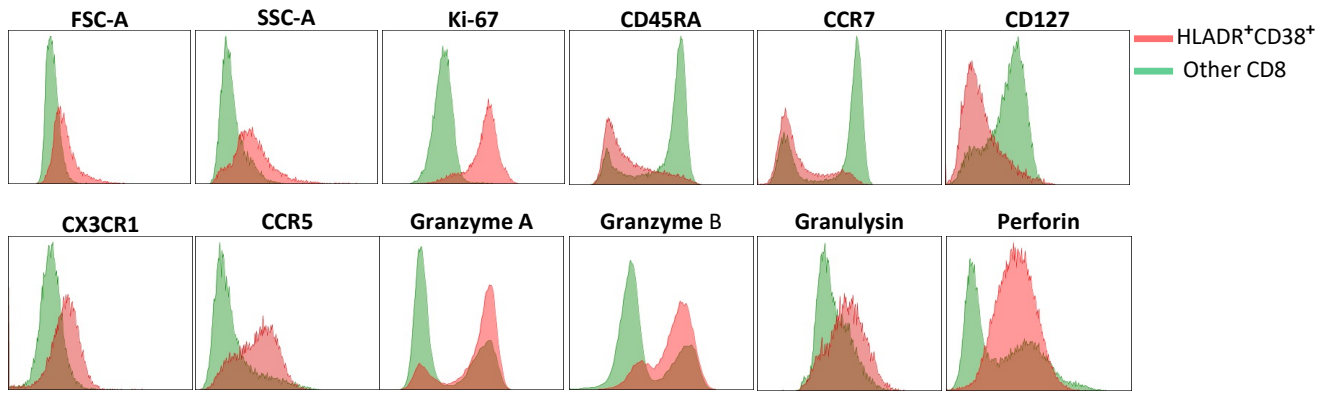
Total no. of patients	100
No. of males/females	57/43
Age (yr) [range (avg)]	25.5 (15-66)
No. of days post-onset of clinical symptoms [range (avg)]	3-12 (7.5)

---

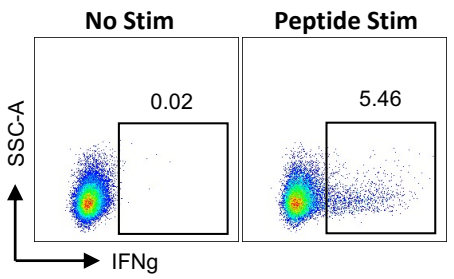
**A.**



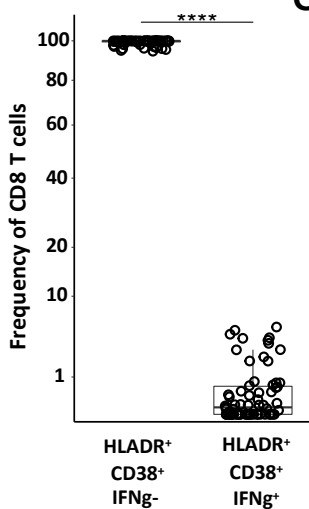
**D.**



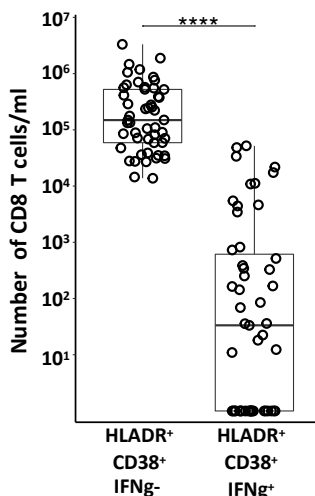
**E.**



**F.**



**G.**



**H.**

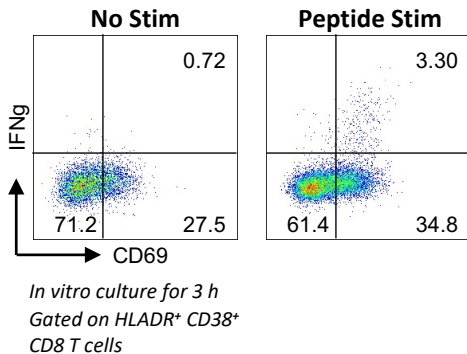
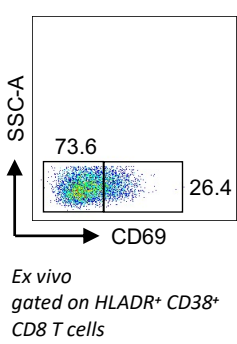
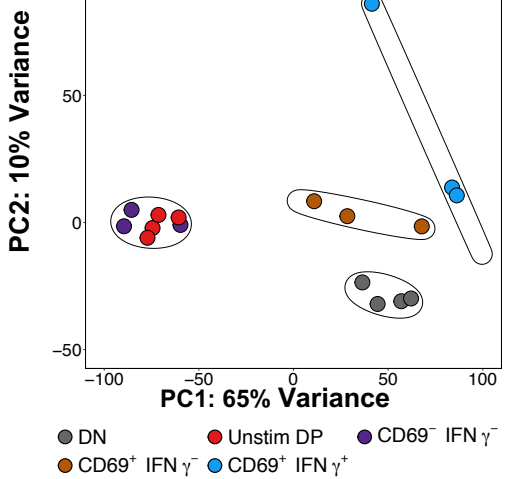
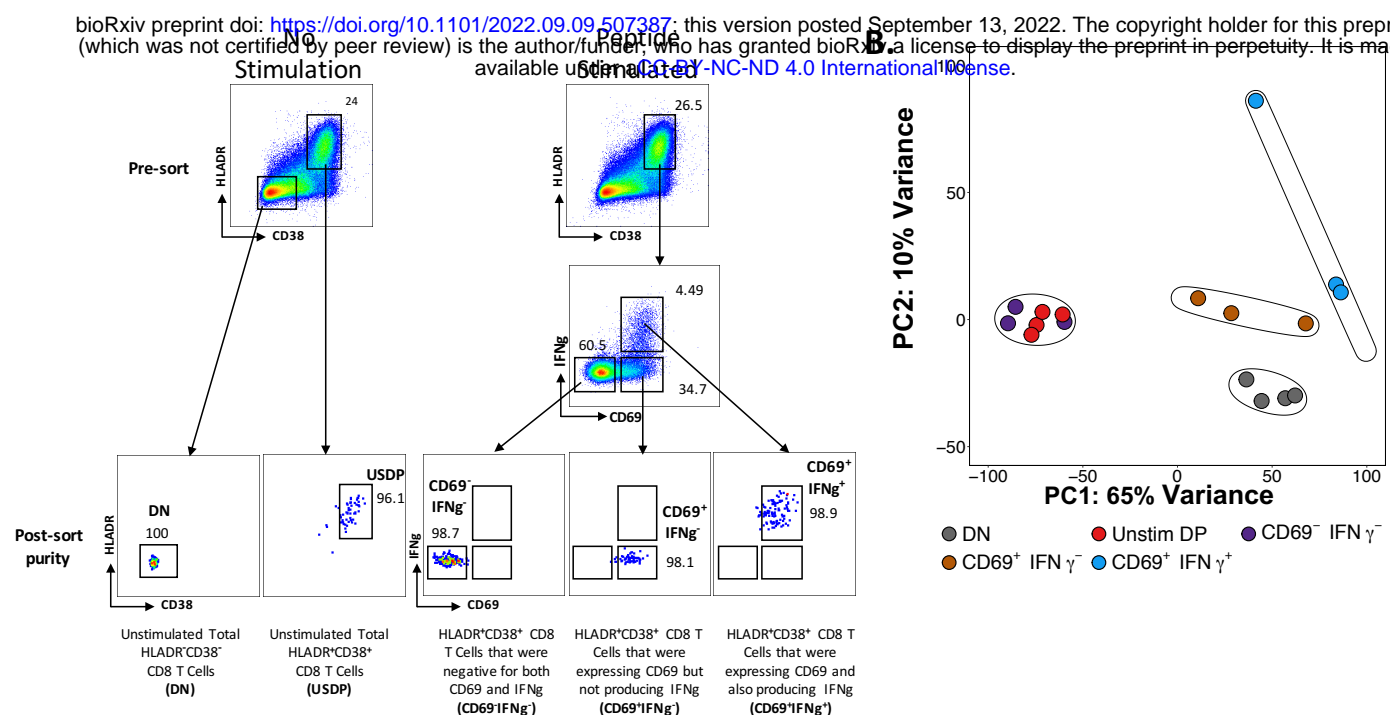
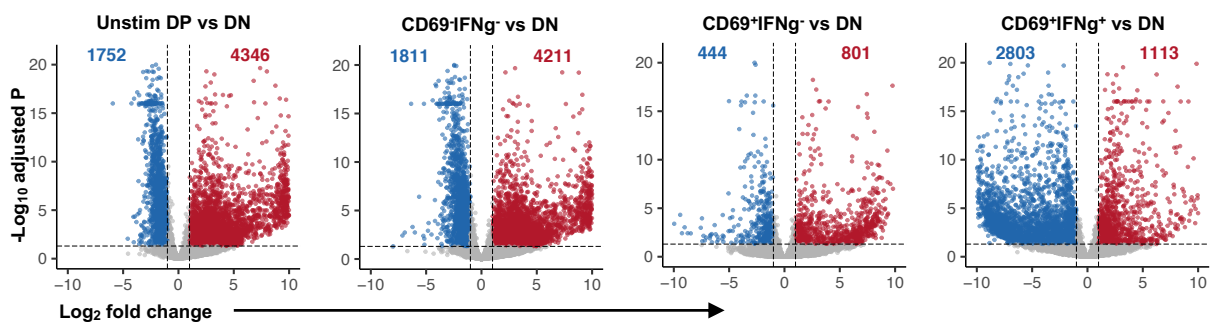


**Figure 1**

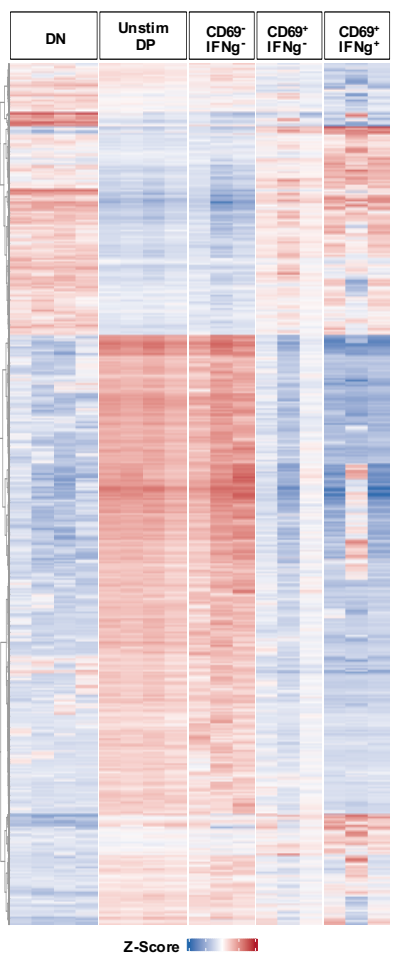
**A.**



**C.**



**D.**



**E.**

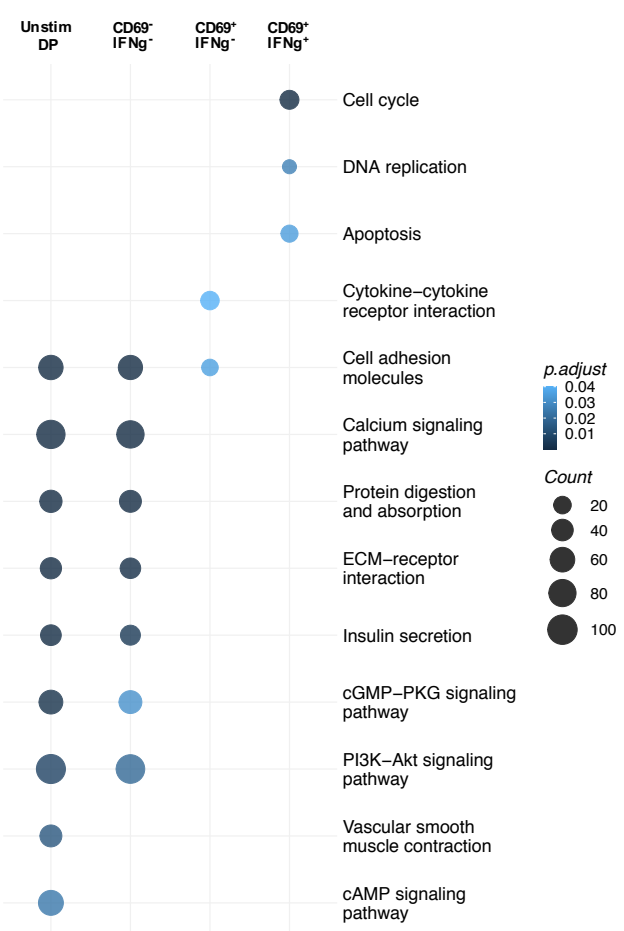
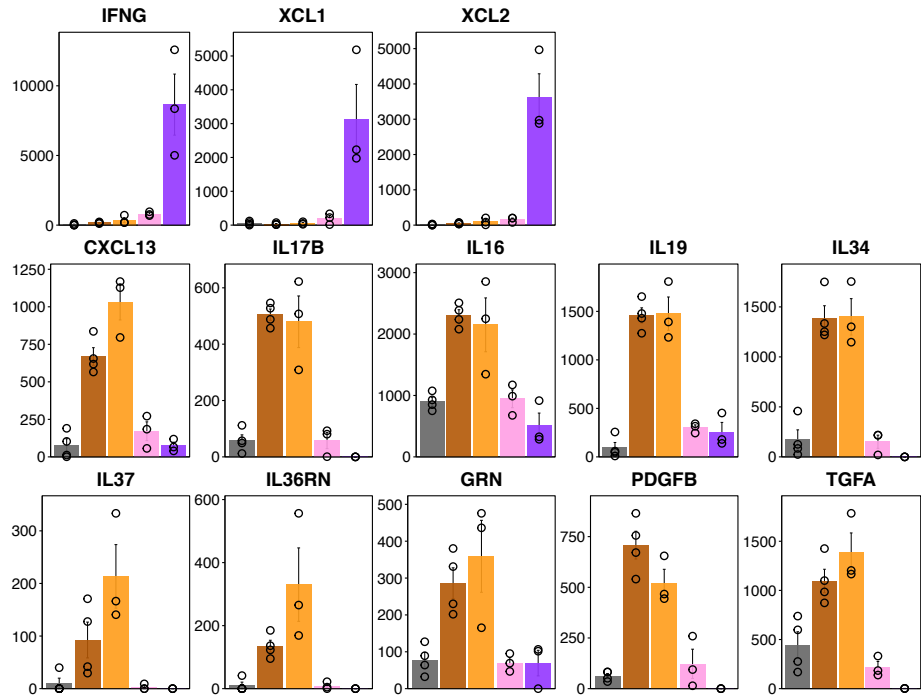
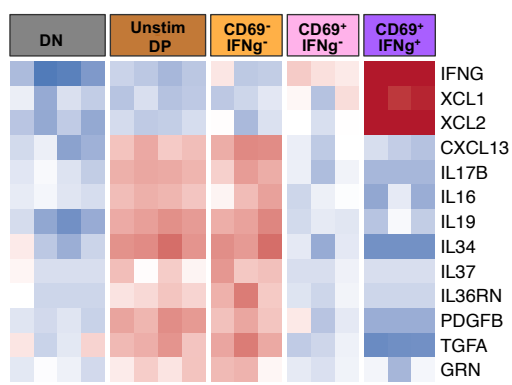


**Figure 2**

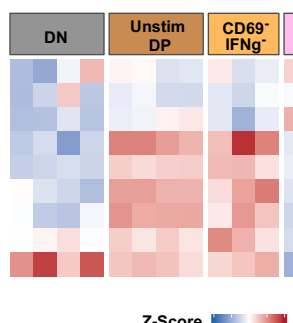
**A.**

### Cytokines and Chemokines



**B.**

### Cytokines and Chemokines receptors



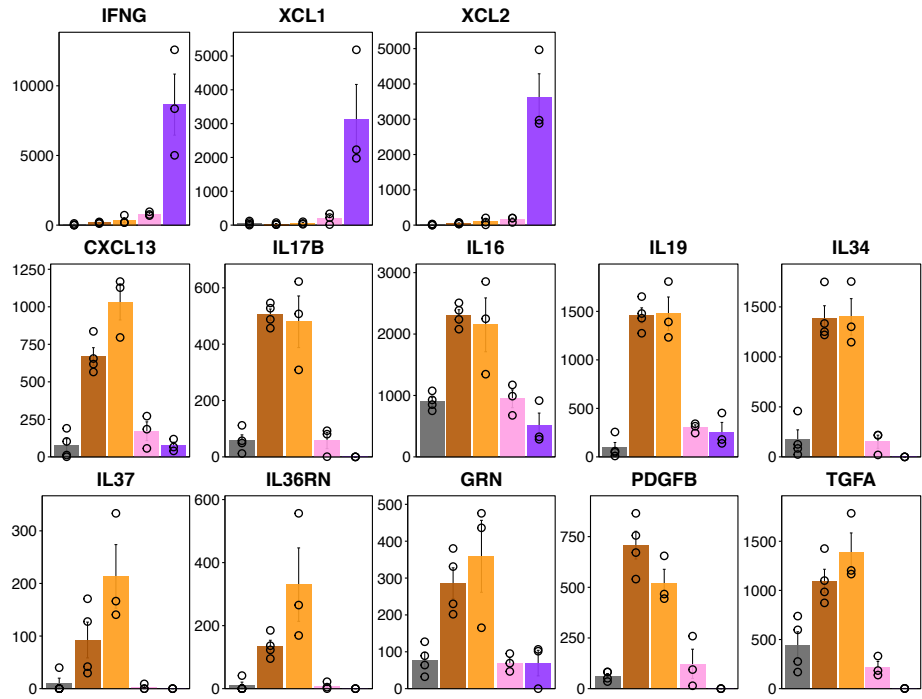
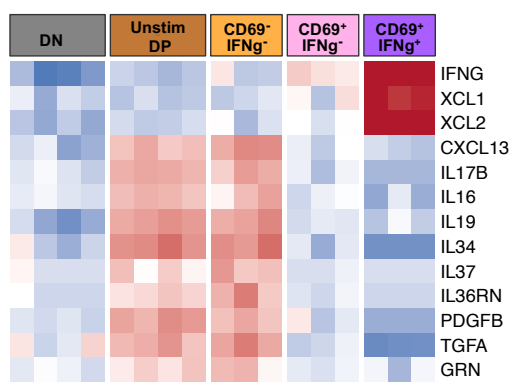
Legend for cell types:

- DN (Dark Gray)
- Unstim DP (Brown)
- CD69<sup>-</sup> IFNg<sup>-</sup> (Orange)
- CD69<sup>+</sup> IFNg<sup>-</sup> (Pink)
- CD69<sup>+</sup> IFNg<sup>+</sup> (Purple)

**Figure 3**

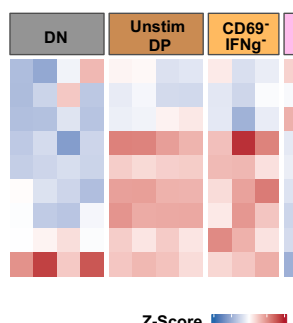
**A.**

### Cytokines and Chemokines



**B.**

### Cytokines and Chemokines receptors



Legend for cell types:

- DN (Dark Gray)
- Unstim DP (Brown)
- CD69<sup>-</sup> IFNg<sup>-</sup> (Orange)
- CD69<sup>+</sup> IFNg<sup>-</sup> (Pink)
- CD69<sup>+</sup> IFNg<sup>+</sup> (Purple)

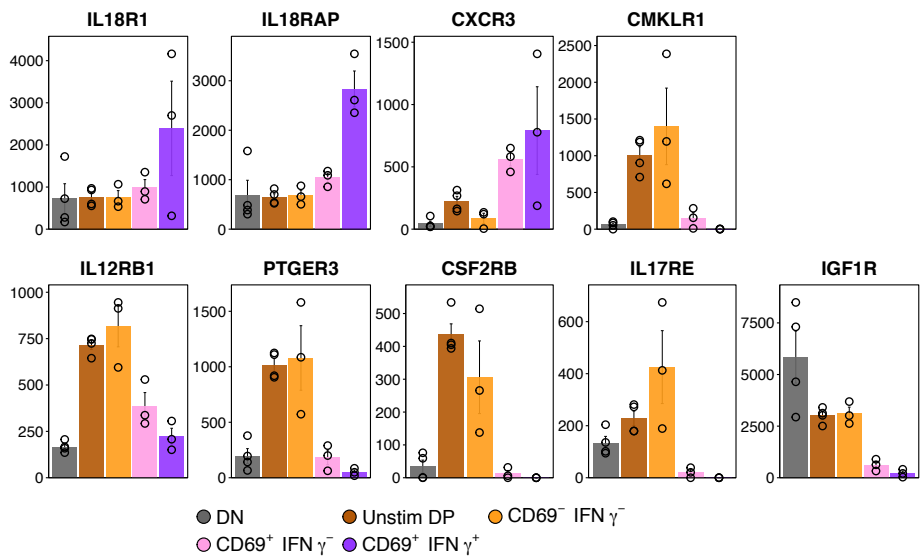
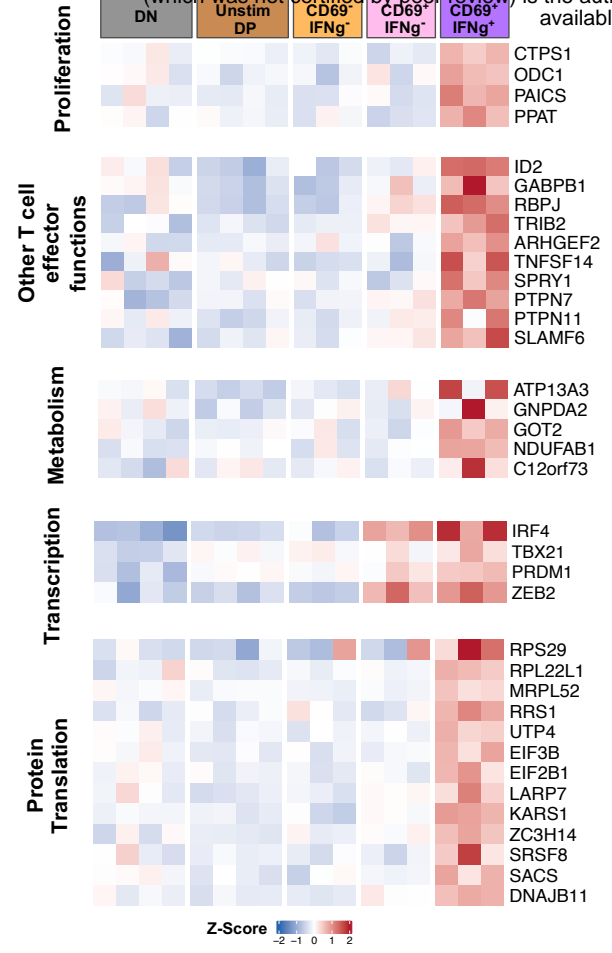
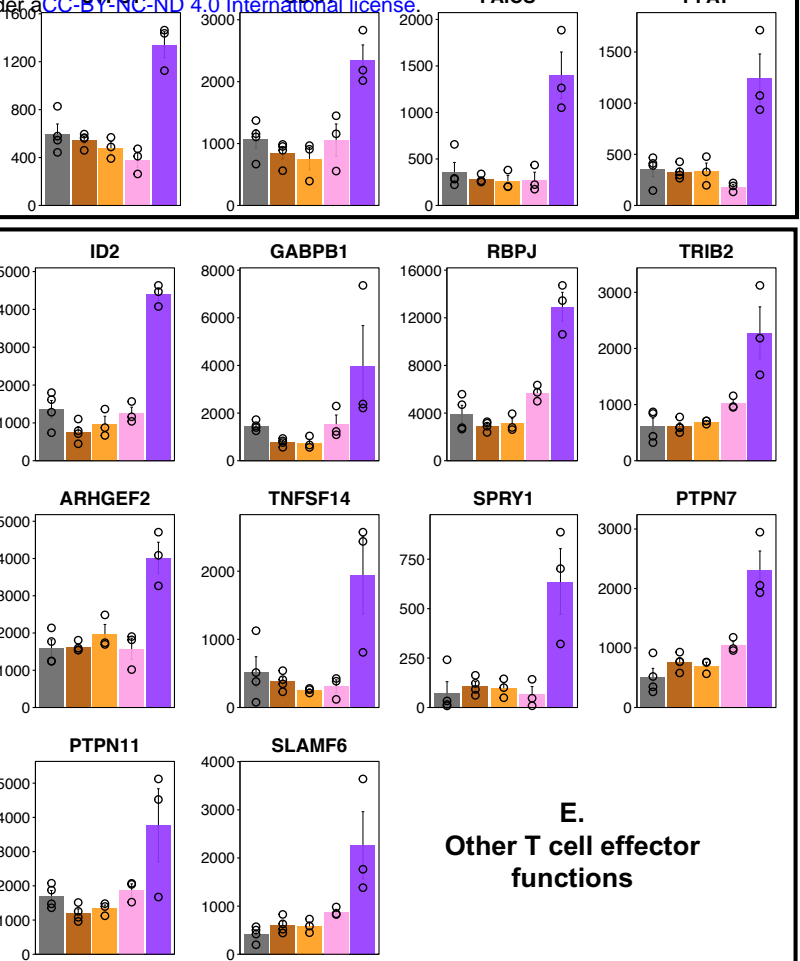


**Figure 3**

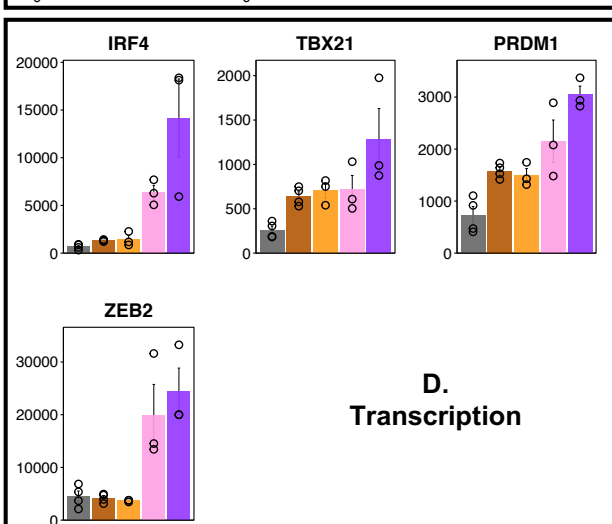
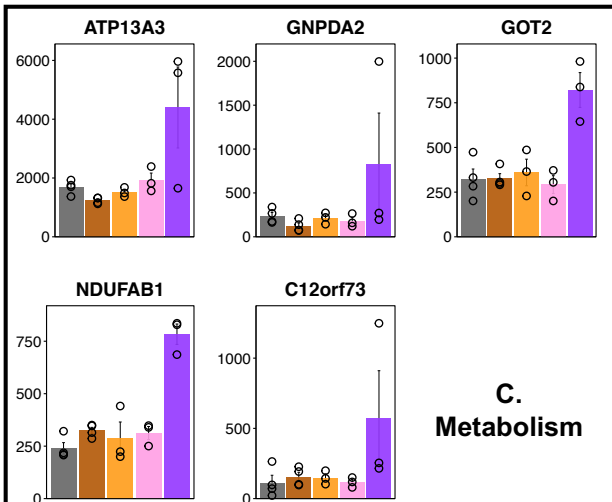
**A**



**B. Proliferation**



**E. Other T cell effector functions**



**F. Protein Translation**

● DN      ● Unstim DP      ● CD69<sup>-</sup> IFN $\gamma$ <sup>-</sup>  
 ● CD69<sup>+</sup> IFN $\gamma$ <sup>-</sup>      ● CD69<sup>+</sup> IFN $\gamma$ <sup>+</sup>

**Figure 5**

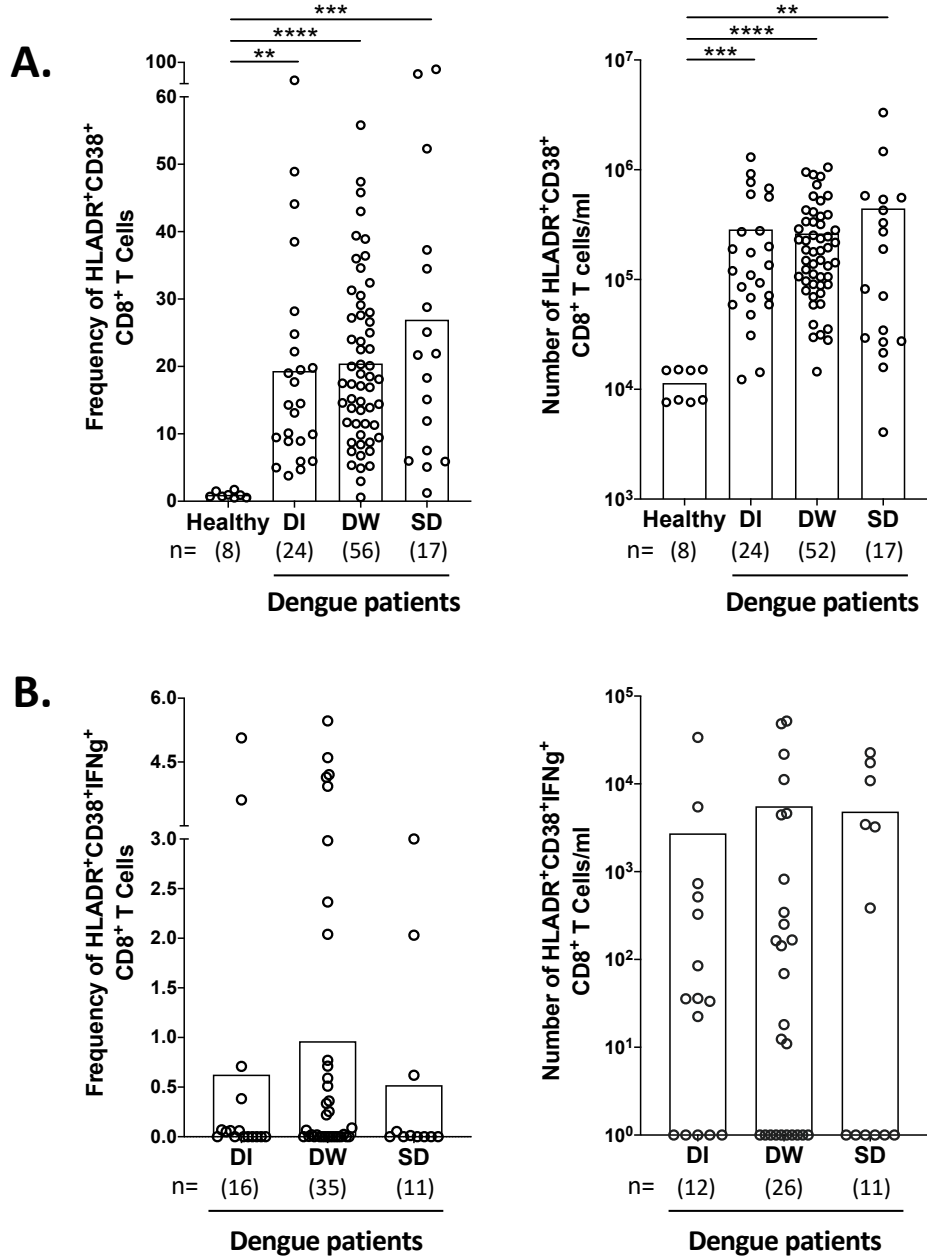


Figure 7